Asymptotic theory of traffic jams

B. S. Kerner,[1] S. L. Klenov,[2] and P. Konhäuser[1]
[1]*Research Institute, Daimler-Benz AG, F1V/V, HPC: E224, 70546 Stuttgart, Germany*
[2]*Department of Physics, Moscow Institute of Physics and Technology, Dolgoprudny, Moscow Region 141700, Russia*
(Received 4 October 1996; revised manuscript received 31 March 1997)

Based on singular perturbation methods, an asymptotic theory of traffic jams of large amplitude is developed. Simple equations describing the form of traffic jams of large amplitude are found. The theory leads to analytical formulas for the *characteristic*, i.e., intrinsic or unique, parameters of traffic flow (such as the average velocity of the downstream front of a wide jam, as well as the flux, density and average vehicle speed of the outflow from the jam) which are independent of the road length, the vehicle density of the initial traffic flow, or other initial conditions. Analytical investigations have been made that show that, in agreement with earlier numerical results [B. S. Kerner and P. Konhäuser, Phys. Rev. E **50**, 54 (1994)], the boundary (threshold) flux at which a traffic jam can still exist is equal to the flux in the outflow from a jam. The manner in which the shape of a traffic jam evolves due to changes in the initial vehicle density is analytically investigated. Simple analytical formulas are obtained for the parameters of narrow traffic jams capable of forming in a limited interval of vehicle densities. A comparison is also made between the results of the present analytical theory of traffic jams, the theory of shock waves in gas dynamics, the classical Lighthill-Whitham-theory [M. J. Lighthill and B. G. Whitham, Proc. R. Soc. London Ser. A **229**, 317 (1955)] of kinematic waves, and the recently discovered experimental features and characteristics of wide traffic jams in actual traffic.
[S1063-651X(97)06710-X]

PACS number(s): 47.54.+r, 05.40.+j, 89.40.+k

I. INTRODUCTION

Traffic jams usually occur when the density of vehicles in traffic is high enough (e.g., Refs. [1–3]). In particular, Treiterer has found out that a traffic jam could spontaneously occur without obvious reason in a traffic flow and that an occurrence of the jam has been accompanied by a hysteresis phenomenon [3]. Recently Kerner and Rehborn have found out from their experimental investigations of ''wide'' traffic jams, i.e., jams that are considerably wider than widths of both upstream and downstream jam's fronts, that the jams have some *characteristic parameters* which do not depend on initial conditions of traffic [4,5]. These characteristic parameters are (i) the mean values of the flux, of the density, and of the average speed of vehicles in the outflow from a wide jam; (ii) the mean value of the density of vehicles inside the jam; and (iii) the average velocity of the jam's downstream front. These parameters can be almost the same for different jams. In addition, for each of wide jams the characteristic parameters can, on average, remain essentially constant over time. Wide jams possess the mentioned properties if the following conditions are fulfilled: (i) traffic parameters (weather, other road conditions, etc.) remain essentially constant; and (ii) there are no hindrances for traffic in the outflow from a wide jam, exactly, if a ''free'' traffic flow, where vehicles are able to change a lane and to pass, is formed in the outflow from the wide jam [4,5].

The existence of characteristic parameters of traffic flow was first predicted, and theoretically investigated, by Kerner and Konhäuser [6] in their numerical and qualitative analyses of a macroscopic traffic flow model based on the ''Navier-Stokes-like'' equation for a traffic flow [7]. Besides a kinetic (macroscopic) approach to the study of traffic flows (e.g., Refs. [7–18]), there is also a ''microscopic'' approach, in which the behavior of each individual vehicle is taken into account (e.g., Refs. [1,19–27]). Various microscopic traffic flow models, as well as macroscopic traffic models, show a transition from an initially homogeneous to a jammed state [6,7,14–18,21–32]. A review of different traffic flow models can be found in the book by Helbing [28]. In particular, qualitative results of investigations of jams by Komatsu and Sasa [33] based on the microscopic dynamical traffic flow model of Bando *et al.* [26] are in agreement with the earlier conclusions, made by Kerner and Konhäuser [6], that the parameters of the downstream front of wide traffic jams represent the characteristics, i.e., intrinsic (unique) parameters, of a traffic flow. It should be noted that the property of jams that some of their parameters are the characteristic parameters of a system is also common for the *autosolitons* formed in many active physical, chemical, and biological systems (for a review, see Refs. [34,35]). A comparison between the properties of jams and the properties of the autosolitons in physical systems was given in Ref. [36].

In this paper an asymptotic theory of large-amplitude traffic jams which are commonly observed in experimental investigations will be developed based on the mathematical method of singular perturbations. The asymptotic theory of jams will be presented in Sec. II. In Sec. III, simple formulas for the characteristic parameters of a traffic flow are derived based on this theory. An analytical investigation of evolving of jams will also be given in this section for a case in which the initial density of vehicles is changed. Section IV contains a comparison between the jam properties found in the presented theory, on the one hand, and the properties of shock waves in gas dynamics (e.g., Ref. [37]), the properties of kinematics waves [38], and the experimental features of traffic jams [4], on the other hand.

II. SINGULAR PERTURBATION THEORY FOR STATIONARY MOVING JAMS

A. Macroscopic traffic flow model

1. Basic equations

If the density of vehicles on a road is not too low and only the average characteristics of their motion are of interest, the traffic flow can be considered as a one-dimensional compressible flow of particles [9–12]. In this kinetic approach a macroscopic model of traffic flow reads [7]

$$\frac{\partial \rho}{\partial t}+\frac{\partial q}{\partial x}=0, \tag{1}$$

$$\rho\left[\frac{\partial v}{\partial t}+v\,\frac{\partial v}{\partial x}\right]=\rho\,\frac{V(\rho)-v}{\tau}-c_0^2\,\frac{\partial \rho}{\partial x}+\mu\,\frac{\partial^2 v}{\partial x^2}, \tag{2}$$

$$v(0,t)=v(L,t),\quad \left.\frac{\partial v}{\partial x}\right|_{0,t}=\left.\frac{\partial v}{\partial x}\right|_{L,t},\quad q(0,t)=q(L,t). \tag{3}$$

To find the characteristic parameters of a wide jam on a road, it is sufficient to analyze the characteristic parameters of a large-amplitude stationary wide jam moving along a circular road. Numerical investigations of jams and their physical attributes [6] indeed demonstrate that the characteristic parameters of both localized wide traffic jams in an open system and the characteristic parameters of stationary wide jams (wide clusters) moving along a circular road are virtually the same. Therefore, boundary conditions (3) can be used with the macroscopic traffic flow model.

In Eqs. (1)–(3) $\rho(x,t)$ is the density $(0<\rho\leqslant\hat{\rho})$ and $v(x,t)$ is the average speed of vehicles $(v\geqslant 0)$, $\hat{\rho}$ is the maximum possible density on the road, $q=\rho v$ is the flux, L is the length of the road, and $V(\rho)$ is the speed-density relationship, i.e., a safe (''maximum and out-of-danger'') speed which is achieved only in a traffic flow that is both time-independent and homogeneous. In a homogeneous state of traffic flow, the density will be designated as ρ_h, the average speed as v_h, $v_h=V(\rho_h)$, and the flux as q_h, $q_h=\rho_h v_h$. $V(\rho)$ is a monotonically decreasing function of ρ, i.e., its derivative [8–12,39]

$$dV(\rho)/d\rho\leqslant 0. \tag{4}$$

In the numerical investigations of jams performed in Refs. [6,16,40–43] and in Sec. IV of this paper, the following function $V(\rho)$ in Eq. (2), which describes the properties of a traffic flow, has been used [7]:

$$V(\rho)=v_f\left[\left\{1+\exp\left(\frac{\rho-\rho_{i0}}{b}\right)\right\}^{-1}-d\right]$$

$$\text{where}\quad d=\left\{1+\exp\left(\frac{\hat{\rho}-\rho_{i0}}{b}\right)\right\}^{-1}. \tag{5}$$

In Eqs. (2) and (5), c_0, μ, τ, v_f, ρ_{i0}, b and $\hat{\rho}$ are constant values which related to the given parameters of traffic (weather, other road conditions, etc.) [6,7,16]. The physical meaning of the equation of motion (2) and of the mentioned parameters of the model have been considered in Refs. [16,40,41].

As in the numerical investigations of jams [6], it will be assumed in this paper that a function $V(\rho)$ and a value c_0 in Eq. (2) provide that there is a finite range of the densities $\rho_{c1}<\rho_h<\rho_{c2}$ that corresponds to a case in which the traffic flow is brought into unstable homogeneous states by an increase in the density. This instability occurs with respect to a growth of small long-wave nonhomogeneous perturbations [44] at a wave number $k=2\pi/L$ [7]. The condition for this instability is [7,45]

$$\left[-1-\frac{\rho}{c_0}\,\frac{dV}{d\rho}\right]\rho>\mu\tau\left(\frac{2\pi}{L}\right)^2; \tag{6}$$

therefore, the values ρ_{c1},ρ_{c2} will satisfy the conditions

$$\left[-1-\left.\frac{\rho_{ci}}{c_0}\,\frac{dV}{d\rho}\right|_{\rho_{ci}}\right]\rho_{ci}=\mu\tau\left(\frac{2\pi}{L}\right)^2,\quad i=1,2. \tag{7}$$

2. Equations for stationary moving jams

As already mentioned, the characteristic parameters of wide jams are nearly identical to the parameters of a wide jam moving at a constant velocity v_g along a circular road [6]. To find the equations for such jams, let us substitute a variable $x\Rightarrow x-v_g t$ into Eqs. (1)–(3). In this new system of coordinates, the macroscopic traffic flow model describing objects moving at a velocity v_g takes the form

$$\frac{\partial \rho}{\partial t}+\frac{\partial q^*}{\partial x}=0, \tag{8}$$

$$\rho\left[\frac{\partial v}{\partial t}+(v-v_g)\,\frac{\partial v}{\partial x}\right]=\rho[V(\rho)-v]-c_0^2\,\frac{\partial \rho}{\partial x}+\mu_0\,\frac{\partial^2 v}{\partial x^2}, \tag{9}$$

and conditions (3). In Eq. (8),

$$q^*=\rho(v-v_g). \tag{10}$$

Here and subsequently the coordinate x is measured in units of $l_0=c_0\tau$, the time in units of τ, and the density ρ in units of $\hat{\rho}$; the speed v in units of c_0, the coefficient μ_0 will be defined as

$$\mu_0=\frac{\mu}{c_0^2\tau\hat{\rho}}. \tag{11}$$

It should be noted that in Eq. (9) the coefficient c_0 has been written in dimensionless form, i.e., it is equal to 1. However, this coefficient shall be retained in the formulas in explicit form to provide a convenient comparison with the results of the work [6].

For the time-independent functions $v(x)$ and $\rho(x)$, which describe stationary moving jams in the new system of coordinates, it is possible to deduce from Eqs. (8) and (3) that the value q^*, Eq. (10), is independent of the coordinate x:

$$q^*=\rho(v-v_g)=\text{const}, \tag{12}$$

i.e., that the value of the average speed of vehicles v will alone depend on the x on the right-hand side of the formula

$$\rho=\frac{q^*}{v(x)-v_g}. \tag{13}$$

It should be noted that, in accordance with Eq. (12), the relation between the flux $q=\rho v$ and the density ρ of the stationary moving jam is represented by the linear expression $q=q^*+\rho v_g$. As follows from Eqs. (9) and (13), the corresponding functions $v(x)$ which describe the possible shapes of stationary moving vehicular jams satisfy the equation [6]

$$\mu_0\frac{d^2v}{dx^2}+q^*\left[\frac{c_0^2}{(v-v_g)^2}-1\right]\frac{dv}{dx}+F(v,q^*,v_g)=0 \tag{14}$$

and the boundary conditions

$$v(0)=v(L),\quad \left.\frac{dv}{dx}\right|_0=\left.\frac{dv}{dx}\right|_L, \tag{15}$$

where

$$F(v,q^*,v_g)=\frac{q^*}{(v-v_g)}\left[V\left(\frac{q^*}{(v-v_g)}\right)-v\right]. \tag{16}$$

An additional condition which connects the functions $v(x)$ with the corresponding value of q^* can be deduced from the obvious integral condition [7]

$$\int_0^L \rho(x,t)dx=\rho_h L. \tag{17}$$

If in this condition formula (13) is taken into account for the stationary case under consideration, then

$$\int_0^L \frac{dx}{v(x)-v_g}=\frac{\rho_h L}{q^*}. \tag{18}$$

Together with the boundary conditions (15), Eqs. (14) and (18) pose an eigenvalue problem whose spectrum defines the possible values of the velocity v_g, and whose eigenfunctions $v(x)$ determine the shapes of different jams.

B. Equations for smooth and sharp distributions

Let us consider a case in which the parameter μ_0 in Eq. (14) is small, i.e., $\mu_0\ll 1$. Then, according to the theory of singular perturbations [46], a solution of Eq. (14) can be represented as a combination of *smooth distributions* $\tilde{v}(x',\mu_0)$ characterized by the length 1 (i.e., l_0) and the sharp distributions $\overline{v}(\zeta,\mu_0)$ characterized by the length μ_0 (i.e., $\mu_0 l_0$):

$$v(x)=v^{(m)}(x),\quad v^{(m)}(x)=\tilde{v}^{(m)}(x',\mu_0)+\overline{v^{(m)}}(\zeta,\mu_0),$$
$$m=1,2, \tag{19}$$

where

$$\zeta=(x-x_0)/\mu_0,\quad x'=x-x_0;$$
$$m=1 \text{ for } 0\leqslant x\leqslant x_0 \text{ and } m=2 \text{ for } L\geqslant x\geqslant x_0, \tag{20}$$

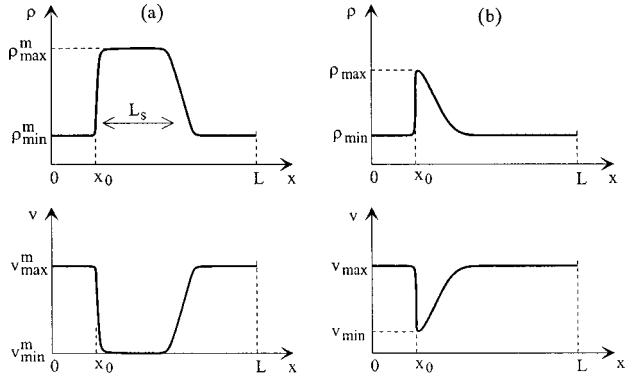

FIG. 1. The qualitative shape of the vehicle density and the average vehicle speed distributions in a wide (a) and in narrow (b) jam stationary moving along a circular road.

and where the point $x=x_0$ is in the region containing the sharp front (Fig. 1). In Eq. (19), the solution for $v(x)$ is represented as a combination of the function $v^{(1)}(x)$ defined on the interval $0\leqslant x\leqslant x_0$ and the function $v^{(2)}(x)$ defined on the interval $L\geqslant x\geqslant x_0$, because the smooth distributions $\tilde{v}^{(1)}(x',\mu_0)$ and $\tilde{v}^{(2)}(x',\mu_0)$ in Eq. (19) can be sufficiently different in the regions upstream and downstream from the sharp front.

According to the singular perturbation theory [46], the functions $\overline{v^{(1)}}(\zeta,\mu_0)$ and $\overline{v^{(2)}}(\zeta,\mu_0)$ exponentially decay with increasing $|\zeta|$, i.e.,

$$\overline{v^{(1)}}(-\infty,\mu_0)=0,\quad \overline{v^{(2)}}(+\infty,\mu_0)=0. \tag{21}$$

Furthermore, at the point $x=x_0$, the functions $v^{(1)}(x)$ and $v^{(2)}(x)$ satisfy the boundary conditions

$$v^{(1)}(x_0)=v^{(2)}(x_0),\quad \left.\frac{dv^{(1)}}{dx}\right|_{x_0}=\left.\frac{dv^{(2)}}{dx}\right|_{x_0}. \tag{22}$$

Let us seek the functions $\tilde{v}^{(m)}(x',\mu_0)$, and $\overline{v^{(m)}}(\zeta,\mu_0)$ involved in Eq. (19), and the values v_g and q^* in series form:

$$\tilde{v}^{(m)}(x',\mu_0)=\tilde{v}_0^{(m)}(x')+\mu_0\tilde{v}_1^{(m)}(x')+\mu_0^2\tilde{v}_2^{(m)}(x')+\cdots,\quad m=1,2, \tag{23}$$

$$\overline{v^{(m)}}(\zeta,\mu_0)=\overline{v_0^{(m)}}(\zeta)+\mu_0\overline{v_1^{(m)}}(\zeta)+\mu_0^2\overline{v_2^{(m)}}(\zeta)+\cdots,\quad m=1,2, \tag{24}$$

$$v_g=v_{g,0}+\mu_0 v_{g,1}+\mu_0^2 v_{g,2}+\cdots, \tag{25}$$

$$q^*=q_0^*+\mu_0 q_1^*+\mu_0^2 q_2^*+\cdots. \tag{26}$$

By substituting expansions (19) and (23)–(26) into Eq. (14), into boundary conditions (15), (21), and (22), and into integral condition (18) and then performing the singular perturbation method, it is possible to find, in the zeroth approximation in μ_0, the equation for the smooth distributions $\tilde{v}_0^{(m)}(x')$ (see the Appendix),

$$q_0^*\left[\frac{c_0^2}{(\tilde{v}_0^{(m)}-v_{g,0})^2}-1\right]\frac{d\tilde{v}_0^{(m)}}{dx'}+F(\tilde{v}_0^{(m)},q_0^*,v_{g,0})=0,$$

$$m=1,2, \tag{27}$$

where

$$F(\tilde{v}_0^{(m)},q_0^*,v_{g,0})=\frac{q_0^*}{(\tilde{v}_0^{(m)}-v_{g,0})}\left[V\left(\frac{q_0^*}{(\tilde{v}_0^{(m)})-v_{g,0}}\right)-\tilde{v}_0^{(m)}\right],$$

$$m=1,2, \tag{28}$$

and the equation for the sharp distributions $\overline{v_0^{(m)}}(\zeta)$ is

$$\frac{d^2\overline{v_0^{(m)}}}{d\zeta^2}+q_0^*\left[\frac{c_0^2}{[\overline{v_0^{(m)}}+\tilde{v}_0^{(m)}(0)-v_{g,0}]^2}-1\right]\frac{d\overline{v_0^{(m)}}}{d\zeta}=0,$$

$$m=1,2. \tag{29}$$

The appropriate boundary conditions are

$$\tilde{v}_0^{(1)}(-x_0)=\tilde{v}_0^{(2)}(L-x_0),\quad d\tilde{v}_0^{(1)}/dx'|_{-x_0}=d\tilde{v}_0^{(2)}/dx'|_{L-x_0}, \tag{30}$$

$$\overline{v_0^{(1)}}(0)+\tilde{v}_0^{(1)}(0)=\overline{v_0^{(2)}}(0)+\tilde{v}_0^{(2)}(0),$$

$$d\overline{v_0^{(1)}}/d\zeta|_0=d\overline{v_0^{(2)}}/d\zeta|_0, \tag{31}$$

$$\overline{v_0^{(1)}}(-\infty)=0,\quad \overline{v_0^{(2)}}(+\infty)=0, \tag{32}$$

and the integral condition is

$$\int_{-x_0}^{0}\frac{dx'}{[\tilde{v}_0^{(1)}(x')-v_{g,0}]}+\int_0^{L-x_0}\frac{dx'}{[\tilde{v}_0^{(2)}(x')-v_{g,0}]}=\frac{\rho_h L}{q_0^*}. \tag{33}$$

The manner in which Eqs. (27)–(29) and conditions (30)–(33) are derived is shown in the Appendix. The solution of Eqs. (27) and (29), obtained under the boundary conditions (30)–(32) and the integral condition (33), determines, in the zeroth approximation in $\mu_0 \ll 1$, the shape of a stationary moving jam, its velocity v_g, and the value q^*:

$$v(x)=\tilde{v}_0^{(m)}(x')+\overline{v_0^{(m)}}(\zeta)+O(\mu_0),\quad m=1,2,$$

$$v_g=v_{g,0}+O(\mu_0),\quad q^*=q_0^*+O(\mu_0). \tag{34}$$

The results of numerical investigations [6] indicate that, depending on the density ρ_h, two types of stationary moving jams can be expected: (i) wide jams [Fig. 1(a)] and (ii) narrow jams [Fig. 1(b)]. In contrast to a narrow jam, the distance L_s between the fronts of a wide jam, where the density and the average speed of vehicles vary sharply, is believed to exceed considerably the widths of the both fronts [Fig. 1(a)].

C. Shape of wide traffic jams

1. Sharp distributions

Equation (29) for sharp distributions is a convenient starting point for determining the shape of a wide traffic jam [Fig. 1(a)]. Integrating Eq. (29) with respect to ζ yields an equation of the form

$$\frac{d\overline{v_0^{(m)}}}{d\zeta}-q_0^*\left[\frac{c_0^2}{\overline{v_0^{(m)}}+\tilde{v}_0^{(m)}(0)-v_{g,0}}+\overline{v_0^{(m)}}+\tilde{v}_0^{(m)}(0)-v_{g,0}\right]+B^{(m)}=0,\quad m=1,2, \tag{35}$$

where $B^{(1)}$ and $B^{(2)}$ are constants, and where the constant $-q_0^*[\tilde{v}_0^{(m)}(0)-v_{g,0}]$ is added to the left-hand side of Eq. (35) in order to simplify the subsequent analysis. It follows from Eqs. (35) and (31) that constants $B^{(1)}$ and $B^{(2)}$ in Eq. (35) are equal to each other, i.e., that $B^{(1)}=B^{(2)}=B$. It is thus possible to introduce the variable

$$\overline{v^*}(\zeta)=\begin{cases}\overline{v_0^{(1)}}(\zeta)+\tilde{v}_0^{(1)}(0)-v_{g,0}, & \zeta\leqslant 0\\ \overline{v_0^{(2)}}(\zeta)+\tilde{v}_0^{(2)}(0)-v_{g,0}, & \zeta>0,\end{cases} \tag{36}$$

and to rewrite Eq. (35) in the form

$$\frac{d\overline{v^*}}{d\zeta}=f(\overline{v^*}). \tag{37}$$

In Eq. (37), the function $f(\overline{v^*})$ is

$$f(\overline{v^*})=\varphi(\overline{v^*})-B,\quad \text{where}\quad \varphi(\overline{v^*})=q_0^*(\overline{v^*}+c_0^2/\overline{v^*}). \tag{38}$$

The boundary conditions (32), written in terms of the variable $\overline{v^*}$ read

$$\overline{v^*}(-\infty)=\tilde{v}_0^{(1)}(0)-v_{g,0},\quad \overline{v^*}(+\infty)=\tilde{v}_0^{(2)}(0)-v_{g,0}, \tag{39}$$

i.e., the solution $\overline{v^*}(\zeta)$ tends to constant values with increasing $|\zeta|$. Equation (37) has solutions which correspond to the boundary conditions (39) only if the function $f(\overline{v^*})$ becomes zero at $\overline{v^*}=\overline{v^*}(-\infty)$ and $\overline{v^*}=\overline{v^*}(+\infty)$ [Eq. (39)], i.e., if there are real solutions, $\overline{v_1^*}=\overline{v^*}(-\infty)$, and $\overline{v_2^*}=\overline{v^*}(+\infty)$, of the equation

$$f(\overline{v^*})=0. \tag{40}$$

The latter is only possible if the constant B in Eq. (38) exceeds the minimum value of the function $\varphi(\overline{v^*})$ in Eq. (38). In this case Eq. (40) has two real roots, $\overline{v^*}=\overline{v_1^*}$ and $\overline{v_2^*}$ [Fig. 2(a)], which are equal to the values $\overline{v^*}(-\infty)$ and $\overline{v^*}(+\infty)$ in Eq. (39), respectively:

$$\overline{v_1^*}=\tilde{v}_0^{(1)}(0)-v_{g,0}\quad\text{and}\quad\overline{v_2^*}=\tilde{v}_0^{(2)}(0)-v_{g,0}. \tag{41}$$

It follows from Eqs. (38) and (40) that the constant B in Eq. (38) can be expressed in terms of the roots $\overline{v_1^*}$ and $\overline{v_2^*}$ as follows:

$$B=q_0^*(\overline{v_1^*}+c_0^2/\overline{v_1^*})=q_0^*(\overline{v_2^*}+c_0^2/\overline{v_2^*}). \tag{42}$$

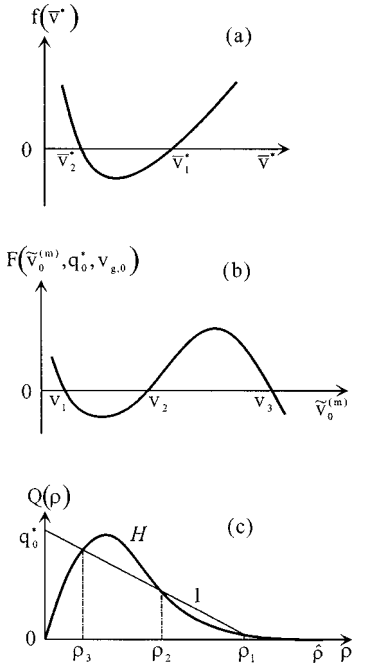

FIG. 2. The qualitative shapes of the function $f(\overline{v^*})$ involved in Eq. (37) (a), of the function $F(\tilde{v}_0^{(m)}, q_0^*, v_{g,0})$, $m=1,2$ and involved in Eq. (27) (b) and the illustrating of a graphical solution of Eq. (47) (c). In (c), curve H is the fundamental diagram $Q(\rho)$, and line 1 corresponds to the function (48) at $q_0^*, v_{g,0}=\text{const}$ and $v_{g,0}<0$.

The second equality in Eq. (42) indicates that the values $\overline{v_1^*}, \overline{v_2^*}$ satisfy the condition

$$\overline{v_1^*} \cdot \overline{v_2^*} = c_0^2. \tag{43}$$

Taking into account Eq. (41), this condition can be written as follows:

$$(\tilde{v}_0^{(1)}(0) - v_{g,0})(\tilde{v}_0^{(2)}(0) - v_{g,0}) = c_0^2. \tag{44}$$

The function $f(\overline{v^*})<0$ at any $\overline{v^*}$ in the interval $\overline{v_1^*} > \overline{v^*} > \overline{v_2^*}$ [Fig. 2(a)]. Therefore, it can be found based on Eq. (37) that the derivative $d\overline{v^*}/d\zeta<0$. This means that only a solution describing a decrease in the average speed of vehicles is the possible solution for the entire class of the sharp distributions. In other words, only the left (upstream) front of a wide jam, where the average speed of vehicles is a decreasing function of the coordinate [Fig. 1(a)], can be described by such sharp distributions. Figure 3(a) shows the shapes of the corresponding sharp distributions $\overline{v_0^{(1)}}(\zeta)$ and $\overline{v_0^{(2)}}(\zeta)$, given as $\overline{v_0^{(m)}}(\zeta) = \overline{v^*}(\zeta) - \tilde{v}_0^{(m)}(0) + v_{g,0}$, $m=1,2$ [see Eq. (36)], where $\overline{v^*}(\zeta)$ is the solution of Eq. (37) under the boundary conditions (39). The sharp distributions $\overline{v_0^{(1)}}(\zeta)$ and $\overline{v_0^{(2)}}(\zeta)$ [Fig. 3(a)], namely, the functions $\overline{v_0^{(1)}}(\zeta) + \tilde{v}_0^{(1)}(0)$ and $\overline{v_0^{(2)}}(\zeta) + \tilde{v}_0^{(2)}(0)$, describe the distribution of the average speed of vehicles in the left (upstream) front of a wide jam [Fig. 1(a)]. In the latter formulas and in Eq. (44), the values $\tilde{v}_0^{(1)}(0)$ and $\tilde{v}_0^{(2)}(0)$ must be determined by an analysis of Eq. (27) for a smooth distribution describing the right (downstream) front of the jam.

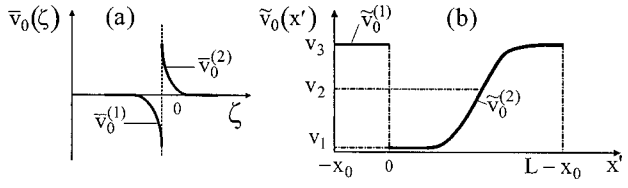

FIG. 3. The qualitative shape of sharp (a) and smooth (b) distributions of the average vehicle speed in a wide stationary moving jam.

2. Smooth distributions

As already mentioned in Sect. II C 1, sharp distributions cannot describe the right (downstream) front of a wide jam, where the average speed of vehicles increases [Fig. 1(a)]. We will demonstrate that this front corresponds to a smooth distribution located in the interval $m=2$ $(0 \leqslant x' \leqslant L - x_0)$. To do this, we will consider the shape of the function $F(\tilde{v}_0^{(2)}, q_0^*, v_{g,0})$ [Fig. 2(b)] given by Eq. (28) for certain constant values q_0^* and $v_{g,0}$. Let us examine first the properties of the roots $\tilde{v}_0^{(2)} = v_i$ of the equation

$$F(\tilde{v}_0^{(2)}, q_0^*, v_{g,0}) = 0 \quad \text{at } q_0^* = \text{const}, \quad v_{g,0} = \text{const}. \tag{45}$$

Using formula (13), namely,

$$\rho = \frac{q_0^*}{\tilde{v}_0^{(2)} - v_{g,0}}, \tag{46}$$

it is possible to write Eq. (45) in the form of equation

$$\rho V(\rho) - \rho v_{g,0} - q_0^* = 0 \quad \text{where } q_0^* = \text{const}, \quad v_{g,0} = \text{const}. \tag{47}$$

The roots $\rho = \rho_i$ of Eq. (47) can be determined as intersection points at which the fundamental diagram $Q(\rho) = \rho V(\rho)$ [curve H in Fig. 2(c)] is intersected by a line

$$\vartheta(\rho, q_0^*, v_{g,0}) = q_0^* + \rho v_{g,0} \tag{48}$$

[straight line 1 in Fig. 2(c)]. It can be seen that there are always functions $Q(\rho)$ and ranges of the values $q_0^* = \text{const}$ and of negative velocities $v_{g,0}<0$ such that the straight line $\vartheta(\rho, q_0^*, v_{g,0})$ intersects the fundamental diagram $Q(\rho)$ at three points ρ_i, $i=1,2,3$ [Fig. 2(c)] and hence Eq. (47) has three roots $\rho = \rho_i$, $i=1,2,3$. As it follows from Eqs. (45), (46), and (28), the relation between the roots $\rho = \rho_i$ (where $i=1,2,3$) of Eq. (47) and three corresponding roots of Eq. (45) $\tilde{v}_0^{(2)} = v_i$ (where $i=1,2,3$), is expressed by the formulas

$$v_i = V(\rho_i), \quad i = 1,2,3. \tag{49}$$

where $v_1 < v_2 < v_3$. When determining the shape of the function $F(\tilde{v}_0^{(2)}, q_0^*, v_{g,0})$, Eq. (28), note that the value of function $F(\tilde{v}_0^{(2)}, q_0^*, v_{g,0})$ is equal to the difference $Q(\rho) - \vartheta(\rho, q_0^*, v_{g,0})$, where $\rho = q_0^*/(\tilde{v}_0^{(2)} - v_{g,0})$. Within the density range $\rho_2 < \rho < \rho_1$, when $v_2 > \tilde{v}_0^{(2)} > v_1$, the inequality $Q(\rho) < \vartheta(\rho, q_0^*, v_{g,0})$ holds true [Fig. 2(c)], therefore giving $F(\tilde{v}_0^{(2)}, q_0^*, v_{g,0}) < 0$. Within the density range $\rho_3 < \rho < \rho_2$, when $v_3 > \tilde{v}_0^{(2)} > v_2$, the inequality $Q(\rho) > \vartheta(\rho, q_0^*, v_{g,0})$

holds true [Fig. 2(c)], therefore giving $F(\tilde{v}_0^{(2)},q_0^*,v_{g,0})>0$. Hence, the function $F(\tilde{v}_0^{(2)},q_0^*,v_{g,0})$ has the shape shown in Fig. 2(b).

It follows from Eq. (49) that the points v_i, $i=1,2,3$ are located on the fundamental diagram, i.e., they may correspond to homogeneous states of traffic flow. It was stated earlier that a homogeneous state of a traffic flow is unstable with respect to long-wave, small-amplitude perturbations within the interval of the density $\rho_{c1}<\rho<\rho_{c2}$, i.e., within the interval of the average speed of vehicles $v_{c1}>v>v_{c2}$, where $v_{ci}=V(\rho_{ci})$, $i=1,2$ [see Eqs. (6) and (7)]. Numerical investigations [6] have proven that the points $\tilde{v}_0^{(2)}=v_1,v_3$ satisfy the conditions $v_1<v_{c2}$ and $v_3>v_{c1}$, i.e., they correspond to a stable state of a homogeneous traffic flow, and that the point $\tilde{v}_0^{(2)}=v_2$ corresponds to an unstable state: $v_{c1}>v_2>v_{c2}$. Therefore, any solution is unstable if it includes an extended essentially homogeneous part for which $\tilde{v}_0^{(2)}\approx v_2$. For this reason such unstable solutions will not be taken into consideration.

The downstream front of a wide jam is a transition layer between a homogeneous traffic flow with a lower average speed of vehicles and another state of homogeneous flow with a higher average speed of vehicles [Fig. 3(b)]. Therefore, this front can only correspond to the solution $\tilde{v}_0^{(2)}(x')$ of Eq. (27) that starts at the point $\tilde{v}_0^{(2)}=v_1$ and ends at the point $\tilde{v}_0^{(2)}=v_3$ [Fig. 3(b), $0\leqslant x'\leqslant L-x_0$]. This means that

$$\tilde{v}_0^{(2)}(0)=v_1,\quad \tilde{v}_0^{(2)}(L-x_0)=v_3. \tag{50}$$

The solution under consideration exists only if the derivative $d\tilde{v}_0^{(2)}/dx'\neq 0$ at the intermediate point $\tilde{v}_0^{(2)}=v_2$, where $F(v_2,q_0^*,v_{g,0})=0$. As follows from Eq. (27), the fulfillment of both conditions

$$d\tilde{v}_0^{(2)}/dx'|_{\tilde{v}_0^{(2)}=v_2}\neq 0,\quad F(\tilde{v}_0^{(2)},q_0^*,v_{g,0})|_{\tilde{v}_0^{(2)}=v_2}=0 \tag{51}$$

can be satisfied at the same point $\tilde{v}_0^{(2)}=v_2$ only when

$$[c_0^2(v_2-v_{g,0})^{-2}-1]=0. \tag{52}$$

Equation (52) yields the following formula for the velocity of a wide jam:

$$v_{g,0}=v_2-c_0 \quad \text{i.e.,} \quad v_{g,0}=V(\rho_2)-c_0, \tag{53}$$

where the expression $v_2=V(\rho_2)$, Eq. (49), has been taken into account. Based on Eq. (27), it can be seen that the derivative $d\tilde{v}_0^{(2)}/dx'$ is positive across the entire interval $v_3>\tilde{v}_0^{(2)}>v_1$, since $F(\tilde{v}_0^{(2)},q_0^*,v_{g,0})>0$ and $[c_0^2(\tilde{v}_0^{(2)}-v_{g,0})^{-2}-1]<0$ at $v_3>\tilde{v}_0^{(2)}>v_2$ and $F(\tilde{v}_0^{(2)},q_0^*,v_{g,0})<0$ and $[c_0^2(\tilde{v}_0^{(2)}-v_{g,0})^{-2}-1]>0$ at $v_2>\tilde{v}_0^{(2)}>v_1$. Hence the solution $\tilde{v}_0^{(2)}(x')$ actually corresponds to the downstream front of a jam, that is, to the area where the vehicle speed increases with increasing x'.

Finally, it can be seen that the solution $v(x)=\tilde{v}_0^{(2)}(x')+\overline{v_0^{(2)}}(\zeta)$ describes the shape of a wide jam at $x_0\leqslant x\leqslant L$ [Fig. 1(a)]. It means that in areas sufficiently removed from the both fronts of the wide jam, where the traffic flow is in one of the homogeneous states, the average speed and the density of the vehicles are equal to the values v_1,v_3 and ρ_1,ρ_3 inside (v_1,ρ_1) and outside (v_3,ρ_3) the jam, respectively.

Let us now consider the function $v(x)=\tilde{v}_0^{(1)}(x')+\overline{v_0^{(1)}}(\zeta)$ which describes a wide jam at $0\leqslant x\leqslant x_0$ [Fig. 1(a)] and determine the shape of a smooth distribution $\tilde{v}_0^{(1)}(x')$. Based on boundary conditions (30) it can be seen that the boundary value $\tilde{v}_0^{(1)}(-x_0)$ of function $\tilde{v}_0^{(1)}(x')$ is equal to $\tilde{v}_0^{(2)}(L-x_0)$, and hence $\tilde{v}_0^{(1)}(-x_0)=v_3$ [see Eq. (50)]. It follows from Eq. (27) that Eq. (27) has no solutions $\tilde{v}_0^{(1)}(x')$ which satisfy the boundary condition $\tilde{v}_0^{(1)}(-x_0)=v_3$, with the exception of the homogeneous solution $\tilde{v}_0^{(1)}(x')=v_3$ [Fig. 3(b)]. To prove this, let us take into account that v_3 is the root of Eq. (45), and the function $F(\tilde{v}_0^{(1)},q_0^*,v_{g,0})$ in Eq. (27) is therefore zero at a value of $\tilde{v}_0^{(1)}=v_3$. Let us assume first that a solution $\tilde{v}_0^{(1)}(x')$ corresponds to a decrease in the average speed of vehicles at $x'>-x_0$, i.e., $\tilde{v}_0^{(1)}(x')|_{x'>-x_0}<v_3$. In this case the condition $F(\tilde{v}_0^{(1)},q_0^*,v_{g,0})>0$ is met [Fig. 2(b)]. On the other hand, since $v_3>v_2$ [Fig. 2(b)], one can see based on (52) that the coefficient $[c_0^2(\tilde{v}_0^{(1)}-v_{g,0})^{-2}-1]$ in Eq. (27) is negative for the values $\tilde{v}_0^{(1)}$ near v_3. It thus follows from Eq. (27) that $d\tilde{v}_0^{(1)}/dx'>0$. The latter result contradicts the initial assumption $\tilde{v}_0^{(1)}(x')<v_3$ at $x'>-x_0$. A similar contradiction arises with a solution corresponding to an increase in the average speed at $x'>-x_0$. Therefore, one can conclude that $\tilde{v}_0^{(1)}(x')=v_3$ and that the shape of a wide jam at $0\leqslant x\leqslant x_0$ is indeed described by the solution

$$v(x)=\tilde{v}_0^{(1)}(x')+\overline{v_0^{(1)}}(\zeta)=\tilde{v}_0^{(2)}(L-x_0)+\overline{v_0^{(1)}}(\zeta). \tag{54}$$

This analysis demonstrates that

$$\tilde{v}_0^{(1)}(0)=\tilde{v}_0^{(2)}(L-x_0)=v_3 \quad \text{and} \quad \tilde{v}_0^{(2)}(0)=v_1.$$

As a result, formula (44) can be written as

$$[V(\rho_3)-v_{g,0}][V(\rho_1)-v_{g,0}]=c_0^2, \tag{55}$$

where expressions (49) have been taken into account.

Three equations

$$\rho_i V(\rho_i)-\rho_i v_{g,0}-q_0^*=0,\quad i=1,2,3, \tag{56}$$

which follow from Eq. (47) at $\rho=\rho_i$ $(i=1,2,3)$, and which are used together with Eqs. (53) and (55) can be used to find five values ρ_1, ρ_2, ρ_3, $v_{g,0}$, and q_0^* which determine, to an accuracy of $\mu_0\ll 1$, the parameters of a wide jam. The solutions of these simple equations will be given in Sec. III.

III. PARAMETERS OF JAMS

A. Characteristic parameters of traffic flow

The following designations, some of which are illustrated in Fig. 1(a), will be used for the main parameters of a wide jam, that is, for (i) the densities, average vehicle speeds, and fluxes inside and outside of the jam, (ii) the velocity of the jam, and (iii) the parameter q^*, respectively [Eq. (12)]: (a) $\rho_{\max}^m$, $\rho_{\min}^m$, $v_{\min}^m$, $v_{\max}^m$, $q_{\min}$, and $q_{\max}=q_{\text{out}}$; (b) v_g^m; and (c) q_s^*. These parameters can be determined, to an accuracy of

$\mu_0 \ll 1$, by solving Eqs. (53), (55), and (56) for ρ_1, ρ_2, ρ_3, $v_{g,0}$, and q_0^* to obtain $\rho^m_{\max}=\rho_1$, $\rho^m_{\min}=\rho_3$, $v^m_{\min}=v_1=V(\rho_1)$, $v^m_{\max}=v_3=V(\rho_3)$, $q_{\min}=\rho^m_{\max}v^m_{\min}$, $q_{\max}=\rho^m_{\min}v^m_{\max}$, $v^m_g=v_{g,0}$, and $q^*_s=q^*_0$. Therefore, conditions (53), (55), and (56) make it possible to write simple formulas that determine the desired relationships between all these parameters. In particular, the equations

$$V(\rho^m_{\min})-V(\sqrt{\rho^m_{\min}\rho^m_{\max}})+c_0(1-\sqrt{\rho^m_{\max}/\rho^m_{\min}})=0, \quad (57)$$

$$V(\rho^m_{\max})-V(\sqrt{\rho^m_{\min}\rho^m_{\max}})+c_0(1-\sqrt{\rho^m_{\min}/\rho^m_{\max}})=0 \quad (58)$$

can be used to determine the outside and inside densities $\rho^m_{\min}$ and $\rho^m_{\max}$ of a wide jam. Meanwhile, the velocity of a wide jam v^m_g, the value $q^*=q^*_s$ and the average speed of vehicles inside $v^m_{\min}$ and outside $v^m_{\max}$ the wide jam, and the flux of vehicles escaping the jam q_{out} are given by

$$v^m_g=V(\sqrt{\rho^m_{\min}\rho^m_{\max}})-c_0, \quad (59)$$

$$q^*_s=c_0\sqrt{\rho^m_{\max}\rho^m_{\min}}, \quad (60)$$

$$v^m_{\min}=V(\rho^m_{\max}), \quad v^m_{\max}=V(\rho^m_{\min}), \quad q_{\text{out}}=q_{\max}=\rho^m_{\min}v^m_{\max}. \quad (61)$$

It is also useful to write the formulas expressing the relation between the density $\rho^m_2=\rho_2$ in Eqs. (56) and (53) and the parameters $\rho^m_{\min}$,$\rho^m_{\max}$:

$$V(\rho^m_2)=V(\rho^m_{\min})+c_0(1-\rho^m_2/\rho^m_{\min}), \quad (62)$$

$$\rho^m_2=\sqrt{\rho^m_{\max}\rho^m_{\min}}. \quad (63)$$

It should be noted that formulas (57)–(63) are correct to $\mu_0 \ll 1$.

It can be seen in Eqs. (57)–(61) that if the function $V(\rho)$ and the value c_0 are given, then the wide-jam parameters $\rho^m_{\max}$, $\rho^m_{\min}$, $v^m_{\min}$, $v^m_{\max}$, q_{out}, v^m_g, and q^*_s may be determined *uniquely*. These parameters are independent of the vehicle density ρ_h, other initial conditions, or road length L. These parameters are therefore the *characteristic* (i.e., intrinsic) parameters of a traffic flow, as is also confirmed by a numerical investigation [6]. These characteristic parameters are merely the functions of the traffic parameters determining the function $V(\rho)$ and value c_0 in Eq. (2).

The characteristic parameters determined by formulas (57)–(61) of the present theory appear to be in good agreement with the results of the numerical investigations of jams [6]. The parameters of traffic flow [values b, v_f, and ρ_i in Eq. (5), and c_0 in Eq. (2)] used in Ref. [6] and contained in Eqs. (57)–(61) do indeed make it possible to find $\rho^m_{\max} \cong 0.683\hat{\rho}$, $\rho^m_{\min}\cong 0.141\hat{\rho}$, $v^m_{\min}\cong 0$, $v^m_{\max}\cong 1.75 l_0/\tau$, $q_{\text{out}} \cong 0.246\hat{\rho} l_0/\tau$, $v^m_g\cong -0.454 l_0/\tau$, and $q^*_s\cong 0.310\hat{\rho} l_0/\tau$. The parameter μ_0, Eq. (11), of the asymptotic theory is equal in this case to $\mu_0\cong 0.162$, i.e., it is not very small. Nevertheless, one can see that these values of the characteristic parameters of traffic flow are very close to $\rho^m_{\max}\cong 0.709\hat{\rho}$, $\rho^m_{\min} \cong 0.144\hat{\rho}$, $v^m_{\min}\cong 0$, $v^m_{\max}\cong 1.73 l_0/\tau$, $q_{\text{out}}\cong 0.250\hat{\rho} l_0/\tau$, $v^m_g\cong -0.439 l_0/\tau$, and $q^*_s\cong 0.313\hat{\rho} l_0/\tau$, respectively, which have been found in the numerical investigation of jams in Ref. [6].

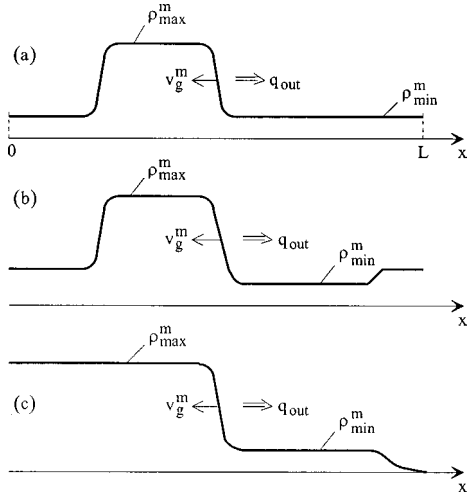

FIG. 4. A qualitative explanation of the characteristic parameters of a traffic flow: Distributions of the density in a wide jam stationary moving along a circular road (a), in a localized cluster of vehicles in an open system (b), and during queue discharge (c). The value $\rho=\rho^m_{\max}$ is the density inside the jams (a) and (b) and in a queue (c). In these three cases the same self-organization process of queue discharge occurs and the same stationary front which moves at a velocity v^m_g ($v^m_g<0$) is formed. In cases (a)–(c), downstream from this front a nearly homogeneous state of a traffic flow is also self-formed, in which the flux is equal to $q=q_{\text{out}}$ and the density is equal to $\rho=\rho^m_{\min}$.

It should be noted that a different unit of length, $l=\sqrt{\mu\hat{\rho}^{-1}\tau}$, was used in Ref. [6], and that in the case under consideration the ratio l_0/l is $l_0/l=2.4845$.

The existence of characteristic parameters of a traffic flow is linked to the following process of self-organization taking place in the downstream front of a wide jam: Drivers escape from a standstill inside the jam at an average rate that is independent of the initial conditions in the traffic flow, such as the density of the initial flow existing prior to jam formation. This self-organizing process depends solely on the traffic parameters, which are function of the controlling parameters of a traffic flow [47].

It should be noted that the self-organizing process involving the escape of vehicles from a standstill inside a wide jam [Fig. 4(a)] is, in essence, a process of queue discharge. Indeed, a jam of sufficient width can be viewed as a regular long queue of vehicles. On the other hand, parameters of the traffic flow upstream from the jam can merely change the length of the queue (the length of the jam), but they have no effect on the escape of vehicles from the jam, i.e., from the queue. Obviously the same stationary process of queue discharge is also realized in the downstream front of a wide jam in the case of a local cluster of vehicles [Fig. 4(b)], and in many other cases involving a possible formation of a long queue of vehicles. In an example of traffic interrupted by traffic lights, a queue discharge occurring when a sufficiently long ''red'' light has changed to the ''green'' light, is identical (after some delay time) (Fig. 4(c)) to a queue discharge from a wide jam [Figs. 4(a) and 4(b)]. In other words, all these different qualitative cases (Fig. 4) involve identical queue discharges in the sense that they are the same self-organizing processes leading to same stationary moving fronts between the queue and the traffic flow downstream

from the queue. As a result of this self-organizing process, the same homogeneous state of traffic flow downstream from the queue is produced, with the flux, density, and average speed of vehicles having the same characteristic parameters q_{out}, $\rho^m_{\min}$, and $v^m_{\max}$ [Fig. 1(a)] as those discussed above.

The width of a wide jam L_s [Fig. 1(a)] is determined by Eq. (33), where the value $q_0^*=q_s^*$ from formula (60) should be used. Therefore, L_s depends on the density ρ_h and road length L. For a given value L, a lower density ρ_h yields a lower value of L_s. This means that at some density ρ_h a wide jam can transform into a narrow jam composed of only two fronts [Fig. 1(b)].

B. Narrow jams

The fronts of a narrow jam can be investigated using a procedure identical to the one used above for wide jams. In this procedure, the characteristic length of change of the average vehicle speed and density is equal to $\mu_0 l_0$, or to l_0, determined by the sharp distribution in the case of the upstream front, and by the smooth distribution in the case of the downstream front, respectively. In contrast to the parameters of a wide jam, the parameters of a narrow jam (narrow cluster) are functions of density ρ_h.

It can be seen that formula (53) can also be used to determine the parameters of a wide jam, but the following formulas should be used for narrow jams instead of formulas (56), (49), and (55), which are valid for wide jams:

$$\rho_i V(\rho_i)-\rho_i v_{g,0}-q_0^*=0, \quad i=2,3,$$

$$\rho_{\max,0}(v_{\min,0}-v_{g,0})-q_0^*=0, \tag{64}$$

$$v_i=V(\rho_i), \quad i=2,3, \tag{65}$$

$$(v_{\min,0}-v_{g,0})[V(\rho_3)-v_{g,0}]=c_0^2, \tag{66}$$

where $\rho_{\max,0}$ is the maximum density and $v_{\min,0}$ the minimum average speed of vehicles in the center of a narrow jam, which are determined to an accuracy of $\mu_0 \ll 1$. It should be noted that formula (66) follows from Eq. (44) if the expressions $\tilde{v}_0^{(2)}(0)=v_{\min,0}$ and $\tilde{v}_0^{(1)}(0)=V(\rho_3)$, which are valid for narrow jams, are used in the latter formula. The narrow-jam parameters such as the maximum and minimum densities $\rho_{\max}$ and $\rho_{\min}$, the maximum and minimum vehicle speeds $v_{\max}$ and $v_{\min}$ [Fig. 1(b)], the jam velocity v_g, and the parameter q^*, calculated to an accuracy of $\mu_0 \ll 1$, are given as $\rho_{\max}=\rho_{\max,0}$, $\rho_{\min}=\rho_3$, $v_{\max}=v_3=V(\rho_3)$, $v_{\min}=v_{\min,0}$, $v_g=v_{g,0}$, and $q^*=q_0^*$, and are thus related to Eqs. (53) and (64)–(66). The external and internal fluxes of a jam apparently are $q_{\text{out}}=q_{\max}=v_{\max}\rho_{\min}$ and $q_{\min}=v_{\min}\rho_{\max}$. However, contrary to the case of a wide jam, the density $\rho_{\max}$ and average speed $v_{\min}$ in the center of a narrow jam do not obey formula (49) at $i=1$. Instead of this formula, the integral condition (33) as well as expressions (53) and (64)–(66) should be used to find the parameters of a narrow jam. For this reason, the parameters of a narrow jam depend on the density ρ_h and road length L.

Of the utmost interest, however, is the case in which the road length L is much larger than the width of a narrow jam, that is, when $L \gg l_0$. In this case the dependence of the narrow-jam parameters on the density ρ_h can be found analytically. To do this, let us write the formulas related to the parameters $\rho_{\min}$, $\rho_{\max}$, v_g, and q^* in terms of ρ_2. According to Eqs. (53) and (64)–(66), the result is [48]

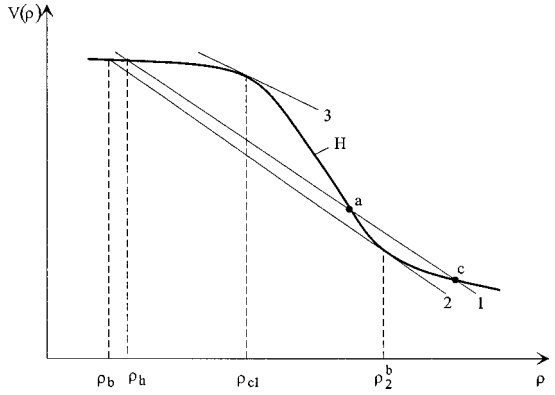

FIG. 5. A qualitative explanation of the solution of Eq. (72): A fragment of the function $V(\rho)$ (curve H); straight lines 1, 2, and 3 correspond to the function $\psi(\rho,\rho_h)$ related to different densities $\rho_h:\rho_b<\rho_h<\rho^m_{\min}$ (line 1), $\rho_h=\rho_b$ (line 2), and $\rho_h=\rho_{c1}$ (line 3).

$$\rho_{\max}=\rho_2^2/\rho_{\min}, \quad V(\rho_2)=V(\rho_{\min})+c_0(1-\rho_2/\rho_{\min}), \tag{67}$$

$$v_g=V(\rho_2)-c_0, \quad q^*=c_0\rho_2. \tag{68}$$

Meanwhile, the integral condition (33) can be written as

$$\rho_{\min}L+\int_0^{L-x_0}[\tilde{\rho}_0^{(2)}(x')-\rho_{\min}]dx'=\rho_h L, \tag{69}$$

where $\tilde{\rho}_0^{(2)}(x')=q_0^*/[\tilde{v}_0^{(2)}(x')-v_{g,0}]$ describes, in terms of the zeroth order of $\mu_0 \ll 1$, the density distribution existing in the downstream front region. Equation (69) can be deduced from Eq. (33) if formulas $\tilde{v}_0^{(1)}(x')=v_3=V(\rho_3)$, and $\rho_{\min}=\rho_3$, and Eq. (64) are taken into account at $i=3$. In view of Eq. (69), it can be seen that the number of vehicles trapped within a narrow jam at $L \gg l_0$ (more particularly, at $L\to\infty$) is negligible in comparison with the total number of vehicles on the road $N=\rho_h L$, i.e., $\rho_{\min}\to\rho_h$ at $L\to\infty$. The function $\tilde{\rho}_0^{(2)}(x')$ does indeed reach $\rho_{\min}$ outside a narrow jam of width l_0, making it possible to ignore the second term on the left-hand side of Eq. (69) at $L\to\infty$ to give $\rho_{\min}=\rho_h$. As a result, the following approximate equations can be obtained from Eq. (67):

$$\rho_{\max}=\rho_2^2/\rho_h, \tag{70}$$

$$V(\rho_2)=V(\rho_h)+c_0(1-\rho_2/\rho_h). \tag{71}$$

C. Boundary (threshold) density and flux of jam's existence

An analysis of Eqs. (70) and (71), shown in Fig. 5, demonstrates that there is a boundary (threshold) density $\rho_h=\rho_b$ which corresponds to a minimum amplitude $\rho_{\max}=\rho_{\max,b}$ [Fig. 6(a)] and a maximum velocity $v_g=v_{g,b}$ of a stable narrow jam [Fig. 6(b)]. This conclusion conforms to the results of the numerical investigation [6]. Indeed, let us first consider solutions of the equation

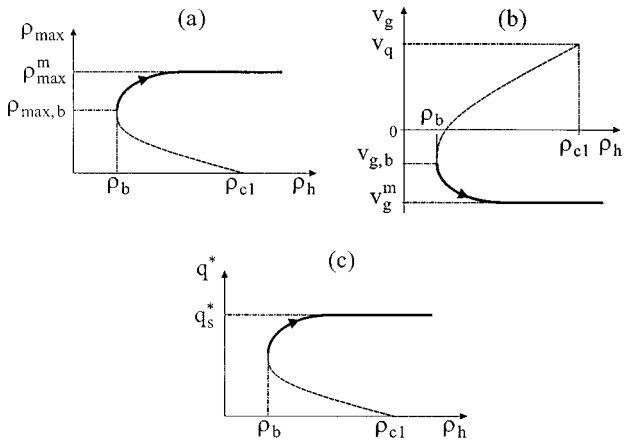

FIG. 6. A qualitative explanation of evolving of a jam for the case in which the density ρ_h is changed: A qualitative shape of dependencies of the jam amplitude ρ_{max} (a), of the jam velocity v_g (b), and of the parameter q^* (c) on the density ρ_h. In (c), $q^*|_{\rho_h=\rho_{c1}}=c_0\rho_{c1}$. Dotted lines correspond to unstable states. The arrows symbolically show a transformation of a narrow stable jam into a wide jam.

$$V(\rho)=\psi(\rho,\rho_h) \quad \text{where} \quad \psi(\rho,\rho_h)=V(\rho_h)+c_0(1-\rho/\rho_h), \tag{72}$$

and where the density ρ_h is a parameter. The roots of Eq. (72), which are obviously the possible values of the density ρ_2 in Eq. (71), can be found as the points at which function $V(\rho)$ (curve H in Fig. 5) intersects with a line $\psi(\rho,\rho_h)$ (straight lines 1, 2, and 3 in Fig. 5).

Equation (72) has two solutions in the density interval (line 1, points a and c, in Fig. 5). Therefore, as follows from Eqs. (70) and (71), there are two different solutions for the density ρ_2 corresponding to two narrow jams with different amplitudes. These two solutions have different parameters and exist at the same density ρ_h (Fig. 6). The greater solution ρ_2 (point c) corresponds to a narrow jam with a higher amplitude, whereas the lesser solution ρ_2 (point a) corresponds to a narrow jam with a lower amplitude. Numerical calculations have shown that the narrow jam of higher amplitude is stable and that the narrow jam of lower amplitude is unstable (Fig. 6).

As the density ρ_h decreases, the larger solution ρ_2 of Eq. (72) decreases and the lower solution ρ_2 increases; therefore, according to Eq. (70), the amplitude of the stable jam of higher amplitude decreases, and the amplitude of the unstable jam of lower amplitude increases. The two solutions of Eq. (72) converge at a density $\rho_h=\rho_b$. The related solution ρ_2 designated in Fig. 5 as $\rho_2=\rho_2^b$. The corresponding line 2 given by $\psi(\rho,\rho_h)$, Eq. (72), is tangent to the function $V(\rho)$. Therefore, density $\rho_h=\rho_b$ and density $\rho_2=\rho_2^b$ can be determined using the equations

$$V(\rho_2^b)=V(\rho_b)+c_0(1-\rho_2^b/\rho_b), \quad dV/d\rho|_{\rho_2^b}=-c_0/\rho_b. \tag{73}$$

The density $\rho_h=\rho_b$ given by Eq. (73) determines the boundary (threshold) density of traffic jam existence, because Eqs. (70) and (71) have no solutions at $\rho_h<\rho_b$, and no solutions therefore exist in the form of traffic jams. The corresponding boundary flux is $q_b=\rho_b V(\rho_b)$. It should be noted that the density is $\rho_{min}=\rho_h$ at $L\to\infty$. Let the value ρ_{min} related to the boundary density $\rho_h=\rho_b$ be designated as $\rho_{min}=\rho_{min,b}$. This value is equal to ρ_b: $\rho_{min,b}=\rho_b$, i.e., it is in agreement with the results of the numerical calculations [6],

$$q_b=q_{out}, \tag{74}$$

where $q_{out}=\rho_{min}V(\rho_{min})$ is the flux in the outflow from the jam. The physical explanation of formula (74) is very simple [6]: if a flux into a jam q_h exceeds q_{out}, the width of the jam L_s increases. Otherwise, if $q_h<q_{out}$, then L_s decreases monotonically, and the jam gradually disappears. Therefore, if $q_h<q_{out}$, then a jam can be neither created nor sustained for a long time, i.e., the boundary flux q_b at which the jam can still be sustained is indeed q_{out}.

As follows from Eqs. (68) and (70), at the boundary density $\rho_h=\rho_b$ the amplitude of the stationary jam $\rho_{max}=\rho_{max,b}$, its velocity $v_g=v_{g,b}$, and the value $q^*=q_b^*$ are given by

$$\rho_{max,b}=(\rho_2^b)^2/\rho_b, \quad v_{g,b}=V(\rho_2^b)-c_0, \quad q_b^*=c_0\rho_2^b. \tag{75}$$

The density ρ_{min} outside a narrow jam is slightly lower than the density ρ^m_{min} outside a wide jam, i.e., $\rho_b<\rho^m_{min}$. Therefore, the flux out from narrow jams q_{out} is also slightly lower than the corresponding flux q_{out} out from a wide jam. As follows from numerical calculations, these fluxes differ only slightly. For this reason, formula (74) is roughly valid even if the value q_{out} for the flux out from a wide jam, Eq. (61), is used in this formula [49].

D. Evolution of narrow jams with increase in density

The analysis in Sec. III C was made for the density range $\rho_b<\rho_h<\rho^m_{min}$, where there are two solutions related to narrow jams: a stable one at a higher amplitude and an unstable one at a lower amplitude [Fig. 6(a)]. As the density ρ_h increases, the amplitude of the stable jam of higher amplitude increases, and the amplitude of the unstable traffic jam of lower amplitude decreases [Fig. 6(a)]. When ρ_h approaches the characteristic density ρ^m_{min}, which is realized outside a wide jam [Fig. 1(a)], the narrow jam of higher amplitude gradually transforms into a wide jam with the amplitude ρ^m_{max} (this transformation is shown schematically with arrows in Fig. 6). A further increase in ρ_h merely increases the width of the jam L_s, but has no effect on the other parameters of the jam, which remain equal to the characteristic parameters determined by Eqs. (57)–(61).

A narrow unstable jam of lower amplitude evolves differently when the density ρ_h is increased. As follows from an analysis of the roots of Eq. (72) (Fig. 5), the higher the density ρ_h, the lower the value ρ_2, which corresponds to a narrow jam of lower amplitude (point a in Fig. 5). Therefore, as follows from formula (70) that the amplitude of a narrow unstable jam ρ_{max} gradually decreases with increasing density ρ_h [dotted line in Fig. 6(a)]. If the density ρ_h is increased further, the value ρ_b merges with the root of Eq. (72) under consideration when the line $\psi(\rho,\rho_h)$, Eq. (72), becomes tangent to the curve $V(\rho)$ (line 3 in Fig. 5). In the point of contact $\rho=\rho_h$ the slope $(dV/d\rho|_{\rho_h})$ of the curve $V(\rho)$ equals

the slope $(-c_0/\rho_h)$ of the line $\psi(\rho,\rho_h)$, Eq. (72); i.e., the condition

$$dV/d\rho|_{\rho_h} = -c_0/\rho_h \tag{76}$$

is fulfilled. A comparison between Eqs. (76) and (7) indicates that this condition determines the critical density $\rho_h = \rho_{c1}$ of stability of a homogeneous traffic flow with respect to global perturbations of small amplitude when $L \to \infty$. Therefore, at $\rho_h \to \rho_{c1}$ the amplitude $\rho_{\max} - \rho_h = \rho_2^2/\rho_h - \rho_h$ of an unstable narrow jam tends to zero [Fig. 6(a)].

It should be noted that Kurtze and Hong [29] found that at a density ρ_h near the critical point $\rho_h = \rho_{c1}$ the form of a low-amplitude unstable traffic jam can be described with the aid of the perturbed Korteweg–de Vries equation deduced in Ref. [29] from the model [Eqs. (1)–(3)]. It can be shown that for a low-amplitude jam the approach based on the singular perturbation theory holds, and that formulas (70) and (71) remain valid if the density ρ_h satisfies the condition $(\rho_{c1} - \rho_h)\rho_{c1}^{-1} \geqslant \mu_0$ (where $\mu_0 \ll 1$), i.e., if $\rho_h \leqslant \rho_{c1} - \mu_0\rho_{c1}$.

The manner in which the jam's velocity v_g and the parameter q^* depend upon the density ρ_h can be determined based on the consideration presented above [Figs. 6(b) and 6(c)]. These dependencies follow from Eqs. (68) and from the formula $v_q = V(\rho_h) - c_0$ (e.g., Ref. [7]) for the phase velocity of small-amplitude perturbations near the homogeneous state of a traffic flow at density $\rho_h = \rho_{c1}$, Eq. (7).

IV. DISCUSSION AND CONCLUSIONS

The asymptotic theory of traffic jams presented here makes it possible to find simple analytical expressions for the main parameters of large-amplitude jams usually observed in experimental observations. An analysis of these analytical expressions shows that, according to the results of numerical [6] and experimental [4] investigations, a traffic flow has characteristic parameters that are independent of the initial conditions of the traffic flow. Good agreement exists between the characteristic parameters derived from the analytical expressions of the present theory and the characteristic parameters obtained in the numerical investigation [6]. These two approaches, that is, the numerical investigation [6] and the analysis of analytical expressions, point to the existence of a boundary (threshold) density ρ_b and a corresponding boundary (threshold) flux q_b of jam formation. If the flux of a traffic flow is lower than q_b, a jam can be neither formed nor sustained for a long time in this traffic flow.

It should be noted that the fronts of a traffic jam (Fig. 1) in which both the density and the average vehicle speed undergo noticeable spatial variations may be viewed as shock waves of a traffic flow. Shock waves also commonly occur in other nonlinear media, and in those associated with gas dynamics in particular [37]. On the other hand, in 1955 Lighthill and Whitham put forth a theory of shock (kinematic) waves in traffic flows [38]. It may be reasonable to compare the traffic-jam properties obtained based on the numerical investigation [6] and the theory presented in this paper, on the one hand, and the results obtained based on the well-known Lighthill-Whitham-theory of traffic flow (Sec. IV B) and the shock waves investigated in gas dynamics (Sec. IV C), on the other hand. Before making this comparison, however, we will briefly consider in Sec. IV A the properties of jams in an actual traffic flow, and compare these experimental properties of jams [4] with theoretical predictions.

A. Comparison of theoretical and experimental results

Based on the experimental observations of a large number of wide jams on numerous German highways, Kerner and Rehborn found that an actual wide jam has the following [4] characteristics.

(i) A jam can move along a highway for a long time while preserving its shape and main parameters.

(ii) A stable localized complex structure consisting of several jams can exist on a highway.

(iii) When the ''controlling'' parameters of traffic are given and ''free'' flow is formed in the outflow from the jam, the averaged fluxes out from various wide jams are roughly equal to each other. The downstream fronts of various wide jams are essentially the same stationary moving structure. Therefore, the mean characteristics (velocity, etc.) of these jam's fronts are virtually constant over time.

(iv) An essentially stationary moving traffic jam can exist on a highway.

(v) The flux of a ''free'' traffic flow can be considerably higher than the flux out from a wide jam.

As follows from the results of the numerical calculation performed in Ref. [6] and from the results of the analytical theory presented in the paper the macroscopic model [Eqs. (1)–(3)] is capable of explaining all the experimental properties of traffic jams (i)–(v) mentioned above. The theory and the experiments have been compared in further detail by numerically simulating the case presented in the article [4] based on the traffic flow model Eqs. (1)–(3) and Eq. (5) (Figs. 7 and 8) [50]. The initial flux distribution and initial average vehicle speed distribution were based on the experimental data obtained at 14:09 (these initial distributions ignored fluctuations and other small changes in the variables) [Fig. 7(a)] [51]. At this time, both jams were already within the highway section under consideration (see Figs. 2 and 3 in Ref. [4]). Figures 7(b) and 7(c) show the manner in which the jams developed between 14:09 and 14:24, when both jams were still within the highway section under consideration [4]. Just as in the experiment (Figs. 2 and 3 in Ref. [4]), both the structures and the characteristics of the two jams (including the velocities of the downstream fronts of jams and the flux out from the jams) remain unchanged during the propagation of the jams along the highway [Figs. 7(b) and 7(c)]. The experimental property (v) of a jam (Fig. 4 in Ref. [4]) is also realized by the model Eqs. (1)–(3) under consideration. The latter can be seen in Fig. 8, where, as follows from numerical calculations, the maximum possible flux in a metastable state of a homogeneous traffic flow $q_{\rm cr}$ (see Ref. [6]) is noticeably higher than the flux out from a wide jam $q_{\rm out}$.

B. Traffic jams and kinematic waves in Lighthill-Whitham theory

An assumption that flux is solely a function of density makes it possible to arrive at the theory of kinematic waves developed by Lighthill and Whitham (LW theory) in 1955 [38] rather than at the model Eqs. (1)–(3), in which the de-

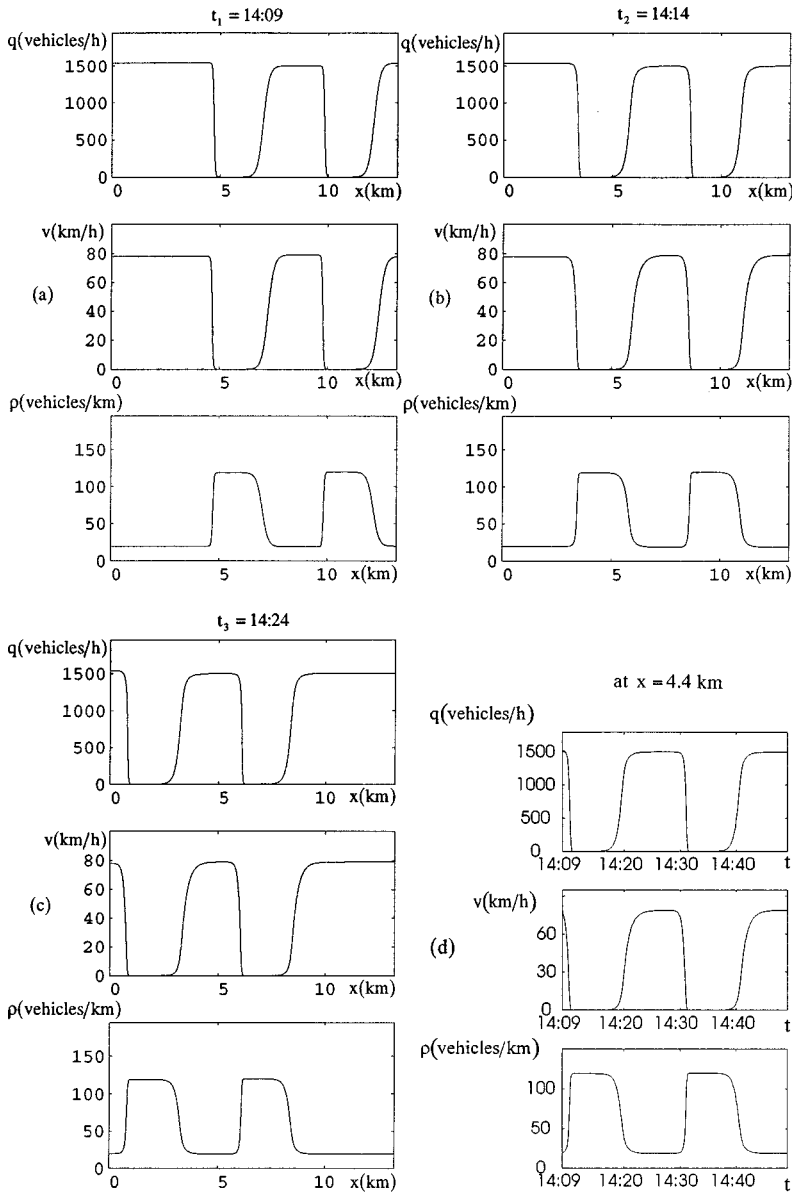

FIG. 7. A comparison of a propagation of jams based on the models (1)–(3) and the experiments made in Ref. [4]: The initial distributions of the flux q, the average speed of vehicles v, and the density ρ (a) and the distributions of these variables during a propagation of the jams along a road (b) and (c). (d) shows the corresponding dependencies $q(t)$, $v(t)$, and $\rho(t)$ at $x=4.4$ km. The parameters of the model are $c_0=39.059$ km/h, $\hat{\rho}=175$ vehicles/km. The function $V(\rho)$ is given by Eq. (5) at $v_f=91.649$ km/h, $\rho_{i0}=0.2\hat{\rho}$, $b=0.05\hat{\rho}$, $d=1.1254\times10^{-7}$, and $\mu_0=0.48$. The characteristic parameters of traffic flow found, i.e., the parameters of the downstream front of the second jam, are $\rho^m_{\max}\simeq120$ vehicles/km, $q_{\text{out}}\simeq1500$ vehicles/h, $v^m_g\simeq-14.6$ km/h, $\rho_b\simeq\rho^m_{\min}\simeq19$ vehicles/km; $v^m_{\min}\simeq0$, and $v^m_{\max}\simeq79$ km/h.

pendence of flux on *both* the density *and* on the average vehicles speed is of crucial importance. Because in the LW theory the flux is related to the density in accordance with the algebraic relation

$$q=Q(\rho) \quad \text{where} \quad Q(\rho)=\rho V(\rho), \tag{77}$$

the equation of motion of vehicles is no longer necessary for the LW model. Hence this model reads

$$\frac{\partial\rho}{\partial t}+c(\rho)\,\frac{\partial\rho}{\partial x}=0 \quad \text{where} \quad c(\rho)=\frac{dQ}{d\rho} \tag{78}$$

and the function $Q(\rho)$ is given by Eq. (77). Solutions provided by the LW model can be waves with group velocity $c(\rho)$ [10,38]. When the density is within a range in which $Q(\rho)$ is convex, regions of lower densities propagate faster than regions of higher densities. Therefore, negative gradients decrease, while positive gradients increase. Ultimately, discontinuities (shocks) appear. If a shock has formed, it moves at the velocity [10,38]

$$v_s=\frac{Q(\rho^+)-Q(\rho^-)}{\rho^+-\rho^-}, \tag{79}$$

where ρ^+ and ρ^- are the densities immediately in front and behind the shock, respectively. The amplitude of the shock fades over time, however [10]. A homogeneous state of traffic flow is finally established. These conclusions are based on the analytical investigations of shocks performed by

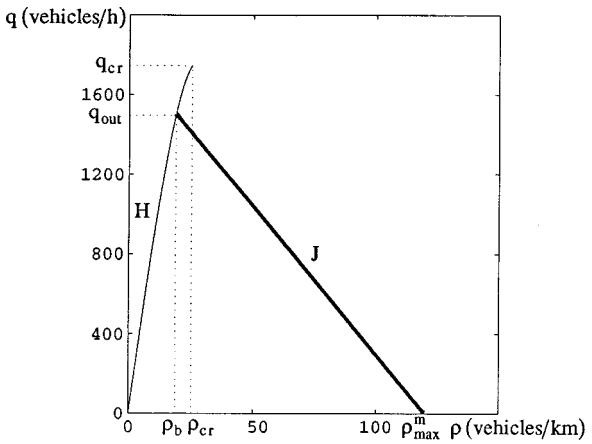

FIG. 8. A representation of the downstream front of the second jam shown in Figs. 7(b) and 7(c) (line J) and of the part of the fundamental diagram (curve H) which corresponds to a stable ($\rho < \rho_b$) and a metastable ($\rho_b \leqslant \rho < \rho_{cr}$) states [6] of a homogeneous traffic flow. Results of the numerical calculations. The model and the parameters are the same as in Fig. 7.

Whitham (see Ref. [10], pp. 46–52). Therefore, any homogeneous state of traffic flow in the LW model is stable because every initial density perturbation will ultimately fade over time [10,38]. In contrast, the model Eqs. (1)–(3) [7] show that, if the flux is higher than the boundary (threshold) value q_b, Eq. (74), a critical localized perturbation grows when its amplitude has exceeded a certain value. This results in the self-formation of traffic jams [6]. The velocity of the downstream front of a wide jam v_g^m, Eq. (59), can be written in the form

$$v_g^m = \frac{Q(\rho^m_{\max}) - Q(\rho^m_{\min})}{\rho^m_{\max} - \rho^m_{\min}}. \tag{80}$$

It is worth mentioning that expression (80) formally corresponds to the shock velocity (79) in the LW theory of kinematic waves. In the LW theory for a traffic flow, however, the densities ρ^+ and ρ^- in Eq. (79) can be arbitrary points on the fundamental diagram $Q(\rho)$ [38]. In contrast, the equation of motion (2), which is given by the model Eqs. (1)–(3) but is absent in the LW theory, plays a *decisive role* in jam formation. Indeed, this equation provides local feedback for a traffic flow [6,7], resulting in the self-formation of traffic jams. This equation also determines the shape of jam fronts and limits the possible shock densities ρ^+ and ρ^- which are related to the downstream front of a wide jam to *the two* distinct values $\rho^+ = \rho^m_{\max}$ and $\rho^- = \rho^m_{\min}$ determined by Eqs. (57) and (58).

The LW model, Eqs. (77) and (78), was numerically simulated to obtain a more complete picture of the behavior of traffic jams in the LW model (Figs. 9–12) [52]. For this purpose, the program and algorithm [53] based on the Godunov's scheme [54,55] were used. In the example shown in Fig. 9 it is assumed that a jam has already formed in a traffic flow by the time $t=0$ [Fig. 9(a), $t=0$]. The jam disappears monotonously as it propagates further along the highway (Fig. 9, $t=5$ and 30 min). Therefore, the LW model depicts a disappearing jam, with the flux upstream from the jam equaling the flux downstream from the jam, whereas the experiments in this case depict the formation of an essentially stationary moving jam on the highway [4]. It can be expected that if the flux upstream from the jam (i.e., the flux into the jam q_{in}) is higher than the flux downstream from the jam (the flux in the outflow from the jam q_{out}), the jam will not disappear and its width will monotonously increase over time. However, the manner in which the jam propagates (Fig. 10) is qualitatively identical to the case described above (Fig. 9), i.e., according to the LW model and contrary to the experiments [4,5], the jam disappears under such conditions (Fig. 10).

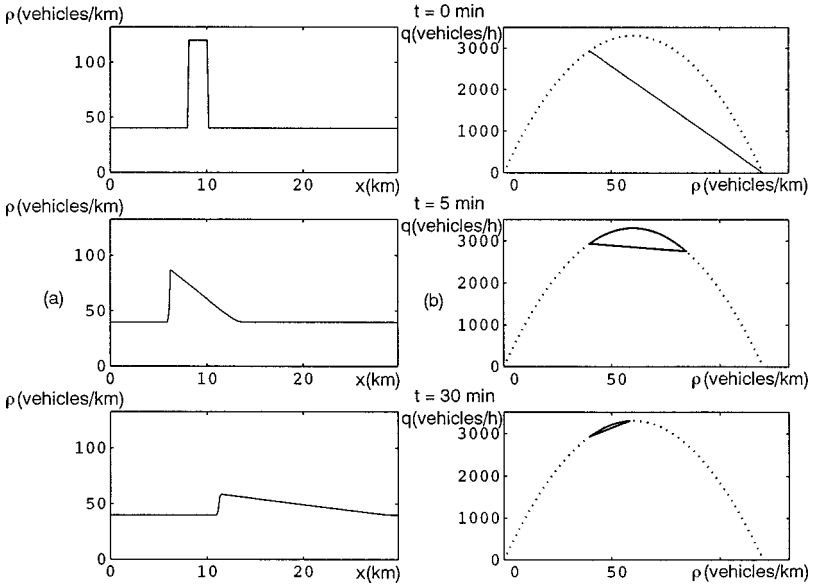

FIG. 9. The propagation of a traffic jam in the LW model (78) with cyclic boundary condition [52]: (a) the distributions of the density in different moments of time; (b) the kinetic of the jam's propagation in the (ρ,q) phase plane. Dotted lines in (b) represent the fundamental diagram $Q(\rho) = \rho v_f(1-\rho/\hat{\rho})$ [10] which was used in the LW model (78), $v_f = 110$ km/h, $\hat{\rho} = 120$ vehicles/km. The initial distribution of the density ($t=0$): the density inside the jam is equal to 120 vehicles/km, the width of the jam is 2 km, and the density outside the jam is equal to 40 vehicles/km.

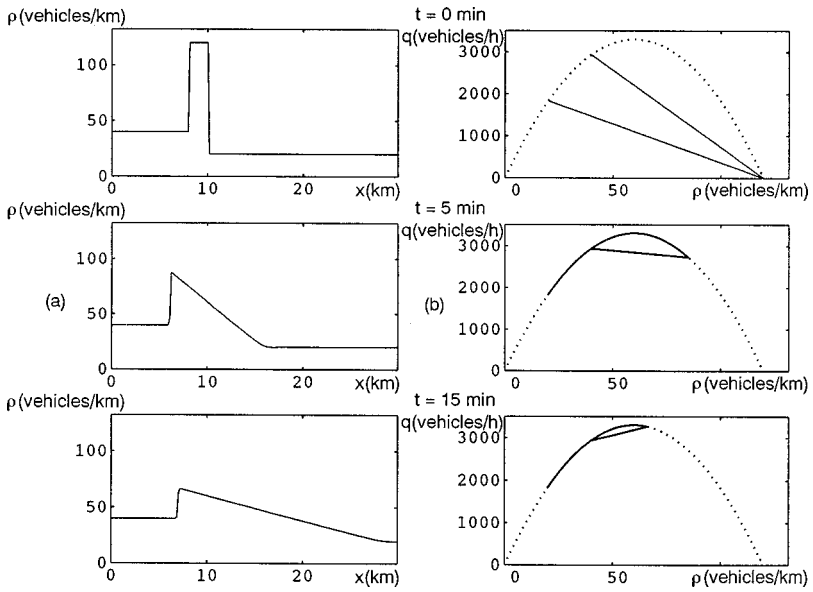

FIG. 10. The propagation of a traffic jam in the LW model (78) when the flux into the jam exceeds the flux out from the jam: (a) the distributions of the density in different moments of time; (b) the kinetic of the jam propagation in the (ρ,q) phase plane. Dotted lines in (b) represent the fundamental diagram. The initial distribution of the density $(t=0)$: the density upstream from the jam is equal to 40 vehicles/km, the density downstream from the jam is equal to 20 vehicles/km. The boundary conditions are $\rho(0,t)=40$ vehicles/km and $\rho(L,t)=20$ vehicles/km. The other parameters are the same as in Fig. 9.

The examples presented in Figs. 9 and 10 correspond to the behavior of a jam described by the LW model having a convex fundamental diagram $Q(\rho)$. When the fundamental diagram $Q(\rho)$ has a concave part (Fig. 11), the initial jam disappears in the same manner as shown in Figs. 9 and 10, although this disappearance has certain distinctive features. In particular, shock waves are formed both upstream and downstream from the jam (Fig. 11, $t=5$ min) [56,57]. Nevertheless, the properties characterizing jam propagation in the LW model [Fig. 11(a)] are *qualitatively* different from the experimental properties of jams (i)–(v) discussed in Sec. II A. For example, the experiments show that a jam's downstream front moves at an essentially constant velocity, whereas the LW model indicates that the velocity v_s of the shock wave, which is related to the downstream front of the jam, varies markedly over time. In particular, the velocity is $v_s \approx -13$ km/h at $t=0$, $v_s \approx -16$ km/h at $t=5$ min, and $v_s \approx -52$ km/h at $t=18$ min (Fig. 11).

For a more detailed comparison of the LW model and the experimental observations, the density distribution experi-

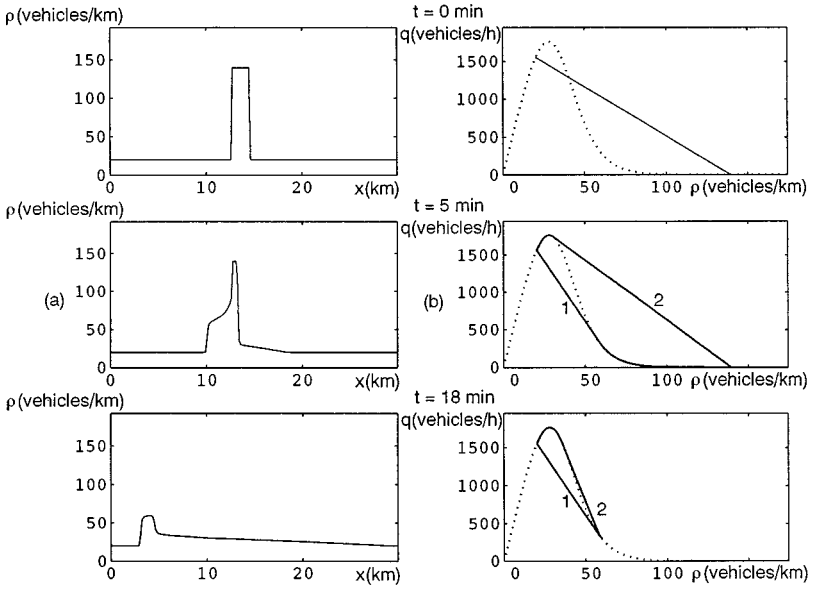

FIG. 11. The propagation of a traffic jam in the LW model (78) with a cyclic boundary condition [52] when the fundamental diagram has a concave part: (a) the distributions of the density in different moments of time; (b) the kinetic of the jam propagation in the (ρ,q) phase plane. Dotted lines in (b) represent the fundamental diagram $Q(\rho)$, which is the same as in Fig. 7. The initial distribution of the density $(t=0)$: the density inside the jam is equal to 140 vehicles/km, the width of the jam is equal to 2 km, and the density outside the jam is equal to 20 vehicles/km.

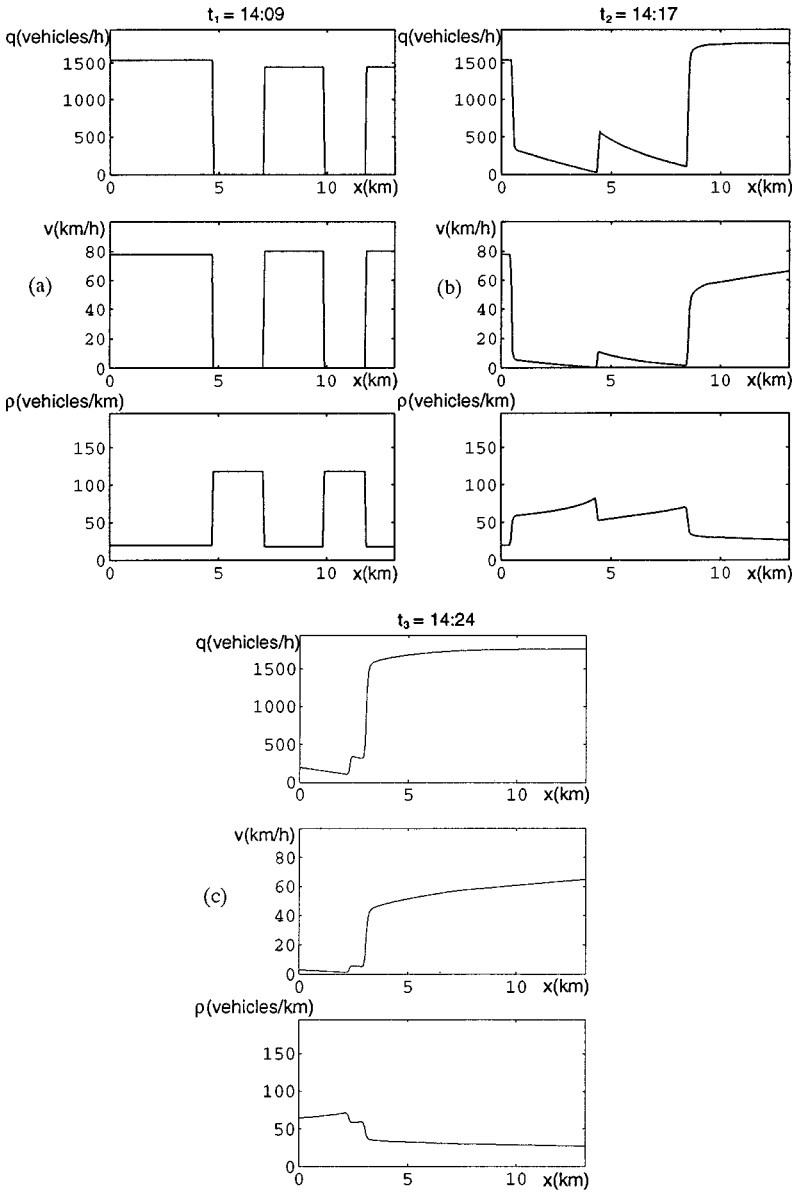

FIG. 12. A comparison of a propagation of jams based on the LW model (78) (see Ref. [52]) and the experiments made in Ref. [4]: (a) The initial distribution of the density ρ and the corresponding distributions of the flux q and of the average speed of vehicles v (b) and (c). The distributions of the density and the corresponding distributions of the flux q and of the average speed of vehicles v during the propagation of jams along a road. The fundamental diagram $Q(\rho)$ is the same as in Fig. 7.

mentally observed (Fig. 2 in Ref. [4]) at 14:09 was used as the initial condition [Fig. 12(a)]. The following results were obtained: (i) In contrast to the experimental observations [4], according to the LW model, the two jams merged in a mere 8 min, at 14:17 [Fig. 12(b)]. The amplitude of the resulting density distribution did not increase following this merger but continued to fade over time in the same manner as in Figs. 9–11. (ii) In contrast to the experimental observations [4], the LW model failed to yield a downstream jam front with an essentially stationary moving structure. In particular, the velocity of the downstream front of the second jam increased in magnitude over time: it was $v_s \approx -14.4$ km/h at 14:09, and $v_s \approx -31$ km/h at 14:15. After the two jams merged, the results were $v_s \approx -41$ km/h at 14:17 and $v_s \approx -52$ km/h at 14:24. (iii) The entire initially localized two-jam structure gradually disappeared according to the LW model but retained its initial properties according to experimental observations [4]. It can thus be concluded that the LW theory of kinematic waves cannot explain properties (i)–(v) of experimentally observed traffic jams (Sec. IV A).

C. Traffic jams and shock waves in gas dynamics

Let us compare the properties of the fronts of traffic jams with the properties of shock waves in gases. Integrating Eq. (14) over the upstream-front region yields

$$\mu_0 \frac{dv}{dx}\bigg|_1^2 - q_s^* \left(\frac{c_0^2}{v - v_g^m} + v - v_g^m \right) \bigg|_1^2 + \int_1^2 F(v, q_s^*, v_g^m)\, dx = 0, \tag{81}$$

where the indexes 1 and 2 correspond, respectively, to the average vehicle speed v upstream ($v = v_{\max}^m$) and downstream ($v = v_{\min}^m$) from the upstream front of a wide jam.

Since the upstream front of the jam is on the order of $\mu_0 \ll 1$ and the derivative dv/dx in the area outside the sharp upstream front is on the order of 1, the first and last terms on left-hand side of Eq. (81) can be ignored to an accuracy of $\mu_0 \ll 1$ to obtain

$$p(\rho^m_{\min})+\rho^m_{\min}(v^m_{\max}-v^m_g)^2=p(\rho^m_{\max})+\rho^m_{\max}(v^m_{\min}-v^m_g)^2. \tag{82}$$

This equation is obtained using formula (12) and the expression $p(\rho)=c_0^2\rho$. Based on Eqs. (12) and (82), the following formula can be obtained:

$$(v^m_{\max}-v^m_g)(v^m_{\min}-v^m_g)=c_0^2, \tag{83}$$

which has already been derived from the asymptotic theory (55).

It should be noted that formula (83) also appears in the well-known gas-dynamic theory of shock waves in the case of polytropic gases (e.g., Ref. [37]). Formulas (12) and (82) do indeed have the form of continuity conditions for the mass and impulse fluxes, respectively, in a reference system moving at velocity $v_g=v^m_g$. The same conditions are met by shock waves in gases [37]. However, the *downstream* front of a jam has no analogy for the continuity condition of an impulse flux. This front is a stationary moving structure formed by self-organizing processes of a traffic flow. The shape and parameters of the downstream front are obtained based on Eq. (27) for a smooth distribution derived under the assumption that the first term in Eq. (14) is negligibly small and can be omitted.

Therefore, there is an important difference between a shock wave in a gas and a traffic jam. The parameters of a shock wave in a gas are determined by the continuity conditions for the mass, impulse, and energy fluxes across the shock wave [37], and are hence dependent upon the parameters of the initial states of the gas upstream and downstream from the wave. In contrast to this, the parameters of the downstream front of a wide jam represent the characteristic parameters of a traffic flow because they are independent of the initial state of the traffic flow. The qualitative difference between the traffic flow approach and the gas-dynamic approach can be understood even better in view of the fact that the parameters of the upstream front of a wide jam in a traffic flow [particularly, the values $v^m_{\max}$ and $v^m_{\min}$ and the front velocity v^m_g in Eq. (83)] cannot be computed without solving Eq. (27) for the downstream front of the jam.

ACKNOWLEDGMENTS

We would like to thank G. Breuel for her fruitful suggestions, and M. Schilke and A. Brenneis for their help in carrying out the numerical calculations.

APPENDIX

In this appendix, Eqs. (27) and (29) are deduced together with conditions (30)–(33) in accordance with the singular perturbation method [46]. Equation (14) can be rewritten in the form

$$\mu_0\frac{d^2v}{dx^2}=q^*\frac{d}{dx}G(v,v_g)-F(v,q^*,v_g), \tag{A1}$$

where

$$G(v,v_g)=v+c_0^2(v-v_g)^{-1}. \tag{A2}$$

Substituting Eq. (19) into Eq. (A1) yields a set of equations

$$\frac{1}{\mu_0}\frac{d^2\overline{v^{(m)}}}{d\zeta^2}+\mu_0\frac{d^2\tilde{v}^{(m)}}{dx'^2}$$

$$=\frac{q^*}{\mu_0}\frac{d}{d\zeta}\overline{G}(\zeta,\mu_0)+q^*\frac{d}{dx'}G(\tilde{v}^{(m)}(x',\mu_0),v_g)$$

$$-\overline{F}(\zeta,\mu_0)-F(\tilde{v}^{(m)}(x',\mu_0),q^*,v_g),\quad m=1,2, \tag{A3}$$

where

$$\overline{F}(\zeta,\mu_0)=F(\overline{v^{(m)}}(\zeta,\mu_0)+\tilde{v}^{(m)}(\mu_0\zeta,\mu_0),q^*,v_g)$$

$$-F(\tilde{v}^{(m)}(\mu_0\zeta,\mu_0),q^*,v_g), \tag{A4}$$

$$\overline{G}(\zeta,\mu_0)=G(\overline{v^{(m)}}(\zeta,\mu_0)+\tilde{v}^{(m)}(\mu_0\zeta,\mu_0),v_g)$$

$$-G(\tilde{v}^{(m)}(\mu_0\zeta,\mu_0),v_g). \tag{A5}$$

Next, Eqs. (23)–(26) are substituted into Eq. (A3) and the nonlinear functions F,G [Eqs. (A4) and (A5)], and $G(\tilde{v}^{(m)}(x',\mu_0),v_g)$, $F(\tilde{v}^{(m)}(x',\mu_0),q^*,v_g)$ are expanded as a series in μ_0 ($\mu_0 \ll 1$). The terms of the same order in μ_0 on the left and right sides of Eq. (A3) are then equated, and the terms dependent on x' and ζ [Eq. (20)], respectively, are separated. As a result, from Eqs. (A3) and (A2) in the zeroth approximation in μ_0 Eqs. (27) and (29) can be deduced. It is taken into account here that

$$\overline{G}(\zeta,\mu_0)=\overline{v_0^{(m)}}(\zeta)+c_0^2(\overline{v_0^{(m)}}(\zeta)+\tilde{v}_0^{(m)}(0)-v_{g,0})^{-1}$$

$$-c_0^2(\tilde{v}_0^{(m)}(0)-v_{g,0})^{-1}+O(\mu_0),\quad m=1,2. \tag{A6}$$

In the zeroth approximation in μ_0, the boundary conditions (30) can be determined based on Eqs. (15), (19) and (21). Substituting expansions (24) into Eq. (21) leads to Eq. (32). Equation (31) is obtained by substituting Eq. (19) and expansions (23) and (24) into Eq. (22), taking Eq. (20) into account, and equating zero-order terms in μ_0. Condition (33) is deduced from Eqs. (18), (19), and (23)–(26), taking into account that functions $\overline{v_0^{(m)}}(\zeta)$ ($m=1,2$) are different from zero only in the region where the sharp upstream front is located. The width of the front is a value on the order of $\mu_0 l_0$. Integration over this region yields only a small contribution in Eq. (18), which should be ignored in the zeroth approximation in μ_0.

[1] R. Herman and K. Gardels, Sci. Am. **35**, 209 (1963).
[2] L. C. Edie and E. Baverez, Report No. RD 65-1, The Port of New York Authority, New York, 1965 (unpublished).
[3] J. Treiterer, Report No. PB 246 094, Ohio State University, Columbus, Ohio, 1975 (unpublished).
[4] B. S. Kerner and H. Rehborn, Phys. Rev. E **53**, R1297 (1996).
[5] B. S. Kerner and H. Rehborn, Phys. Rev. E **53**, R4275 (1996).
[6] B. S. Kerner and P. Konhäuser, Phys. Rev. E **50**, 54 (1994).
[7] B. S. Kerner and P. Konhäuser, Phys. Rev. E **48**, R2335 (1993).
[8] I. Prigogine and R. Herman, *Kinetic Theory of Vehicular Traffic* (American Elsevier, New York, 1971).
[9] H. J. Payne, in *Proceedings of the Mathematical Models of Public Systems* (Simulation Councils, La Jolla, CA, 1971), Vol. 1, Transp. Res. Rec. **68**, 772 (1979).
[10] G. B. Whitham, *Linear and Nonlinear Waves* (Wiley, New York, 1974).
[11] R. Kühne, in *Highway Capacity and Level of Services*, edited by U. Brannolte (Balkema, Rotterdam, 1991), p. 211; and in *9th International Symposium on Transportation Traffic Theory* (VNU Science, 1984).
[12] W. Leutzbach, *Introduction to the Theory of Traffic Flow* (Springer-Verlag, Berlin, 1988).
[13] P. Nelson, Transp. Theory Stat. Phys. **24**, 383 (1995); Transp. Res. B **29**, 297 (1995); D. D. Bui, P. Nelson, and A. Sopasakis, in *Transportation and Traffic Theory*, edited by J-B. Lesort (Elsevier, Oxford, 1996), p. 679.
[14] R. Wegener and A. Klar, Transp. Theory Stat. Phys. **25**, 785 (1996).
[15] H. Lehmann, Phys. Rev. E **54**, 6058 (1996).
[16] B. S. Kerner, P. Konhäuser, and M. Schilke, Phys. Rev. E **51**, 6243 (1995).
[17] M. Hilliges and W. Weidlich, Transp. Res. B **29**, 407 (1995).
[18] D. Helbing, Phys. Rev. E **51**, 3164 (1995); **53**, 2366 (1996).
[19] D. C. Gazis, R. Herman, and R. W. Rothery, Oper. Res. **9**, 545 (1961).
[20] R. Wiedemann, *Simulation des Straßenverkehrsflusses* (Schriftenreihe des Instituts für Verkehrswesen Universität Karlsruhe, 1974), Vol. 8.
[21] K. Nagel and M. Schreckenberg, J. Phys. I (France) **2**, 2221 (1992).
[22] O. Biham, A. A. Middleton, and D. Levine, Phys. Rev. A **46**, 6124 (1992).
[23] T. Nagatani, Phys. Rev. E **48**, 3290 (1993); **51**, 922 (1995).
[24] J. A. Cuesta, F. C. Matínez, J. M. Molera, and A. Sánchez, Phys. Rev. E **48**, 4175 (1993); J. M. Molera, F. C. Matínez, J. A. Cuesta, and R. Brito, *ibid.* **51**, 175 (1995).
[25] H.-T. Fritzsche, Traffic Eng. Control **35**, 317 (1994).
[26] M. Bando, K. Hasebe, A. Nakayama, A. Shibata, and Y. Sugiyama, Phys. Rev. E **51**, 1035 (1995).
[27] *Traffic and Granular Flow*, edited by D. E. Wolf, M. Schreckenberg, and A. Bachem (World Scientific, Singapore, 1996).
[28] D. Helbing, *Verkehrsdynamik* (Springer-Verlag, Berlin, 1997).
[29] D. A. Kurtze and D. C. Hong, Phys. Rev. E **52**, 218 (1995).
[30] M. Y. Choi and H. Y. Lee, Phys. Rev. E **52**, 5979 (1995).
[31] M. Schreckenberg, A. Schadschneider, K. Nagel, and N. Ito, Phys. Rev. E **51**, 2939 (1995).
[32] K. Nagel and M. Paczuski, Phys. Rev. E **51**, 2909 (1995); K. Nagel, in *Traffic and Granular Flow*, edited by D. E. Wolf, M. Schreckenberg, and A. Bachem (World Scientific, Singapore, 1996), p. 41.
[33] T. S. Komatsu and S. Sasa, Phys. Rev. E **52**, 5574 (1995).
[34] B. S. Kerner and V. V. Osipov, Usp. Fiz. Nauk **157**, 201 (1989) [Sov. Phys. Usp. **32**, 101 (1989)]; **160**, 1 (1990) **[33**, 679 (1990)]; B. S. Kerner, in *Nonlinear Dynamics and Pattern Formation in Semiconductors and Devices*, edited by F.-J. Niedernostheide (Springer, Berlin, 1995), p. 70.
[35] B. S. Kerner and V. V. Osipov, *Autosolitons: A New Approach to Problems of Self-Organization and Turbulence* (Kluwer, Dordrecht, 1994).
[36] B. S. Kerner, in *Chaotic, Fractal, and Nonlinear Signal Processing*, edited by R. A. Katz, AIP Conf. Proc. No. 375 (AIP, New York, 1996), p. 777.
[37] L. D. Landau and E. M. Lifshitz, *Hydrodynamics* (Nauka, Moscow, 1986) (in Russia) [English translation of an earlier edition: *Fluid Mechanics* (Pergamon, Oxford, 1959)].
[38] M. J. Lighthill and B. G. Whitham, Proc. R. Soc. London, Ser. A **229**, 317 (1955).
[39] A. D. May, *Traffic Flow Fundamentals* (Prentice-Hall, Englewood Cliffs, NJ, 1990).
[40] B. S. Kerner, P. Konhäuser, and M. Schilke, in *Transportation and Traffic Theory*, edited by J-B. Lesort (Elsevier, Oxford, 1996), p. 119.
[41] B. S. Kerner, P. Konhäuser, and M. Schilke, in *World Transport Research*, edited by D. Hensher, J. King, and T. Hoon Oum (Elsevier, Oxford, 1996), Vol. 2, p. 167.
[42] B. S. Kerner, P. Konhäuser, and M. Rödiger, in *Proceedings of the Second World Congress on Intelligent Transport Systems* (Vertis, Yokohama, 1995), Vol. IV, p. 1911.
[43] B. S. Kerner, P. Konhäuser, and M. Schilke, Phys. Lett. A **215**, 45 (1996).
[44] Note that in the model under consideration, nonhomogeneous perturbations being considered in a system of coordinates moving at velocity v_h can propagate without being noticeably attenuated only toward the upstream side of the source of perturbations. To show this, let us find the solution of the dispersion equation for small amplitude nonhomogeneous perturbations of the form $\propto\exp(ikx-\gamma t)$ derived from Eqs. (1)–(3) in Ref. [7]:

$$\gamma^2-\gamma(2ikv_h+k^2\mu\rho_h^{-1}+\tau^{-1})+ik(k^2\mu v_h\rho_h^{-1}+v_h\tau^{-1}+dV/d\rho|_{\rho_h}\rho_h\tau^{-1})+k^2(c_0^2-v_h^2)=0,$$

where $k=2\pi m/L$, $m=\pm1,\pm2,\ldots$. Using the designations $\lambda=\mathrm{Re}\,\gamma$, $\omega=\mathrm{Im}\,\gamma$, the solution of this equation can be written as

$$\omega=k\{v_h\pm\sqrt{2}|dV/d\rho|_{\rho_h}|\rho_h\tau^{-1}[D_1+(D_1^2+D_2^2)^{1/2}]^{-1/2}\},$$

$$\lambda=\frac{1}{2}\left(\tau^{-1}+k^2\mu\rho_h^{-1}\pm\frac{1}{\sqrt{2}}[D_1+(D_1^2+D_2^2)^{1/2}]^{1/2}\right),$$

where $D_1=(\tau^{-1}+k^2\mu\rho_h^{-1})^2-4k^2c_0^2$, $D_2=-4kdV/d\rho|_{\rho_h}\rho_h\tau^{-1}$. Hence the dispersion equation has a solution with the upper sign + in the formulas for ω and λ which would correspond to small-amplitude, nonhomogeneous perturbations propagating toward the downstream side of the source of perturbations. However, all these nonhomogeneous perturbations rapidly attenuate with higher decrement $\lambda\geqslant1/2\tau^{-1}$. In other words, local perturbations being considered in a system of coordinates moving at velocity v_h can indeed propagate in proper manner solely toward the upstream side of the source of perturbations.
[45] At $L=\infty$, condition (6) transforms to the form found earlier by Whitham [10] and Kühne [11].

[46] R. E. O'Malley, Jr., *Introduction to Singular Perturbation* (Academic, New York, 1974); D. R. Smith, *Singular-Perturbation Theory. An Introduction with Applications* (Cambridge University Press, Cambridge, 1985).

[47] A characteristic of this self-organizing process determining the velocity of the downstream front of a wide jam has recently been proposed by B. S. Kerner [B. S. Kerner, in *Transportation Systems*, edited by M. Papageorgiou and A. Pouliezos (Technical University of Crete, Chania, Greece, 1997), Vol. 2, p. 793.

[48] Note that, as follows from Eqs. (59), (60), (62), and (63), formulas (67) and (68) for narrow jams transform to the formulas for wide jams if the values $\rho_{\min}$, $\rho_{\max}$, v_g, ρ_2, and q^* are replaced by $\rho^m_{\min}$, $\rho^m_{\max}$, v^m_g, ρ^m_2, and q^*_s, respectively. In particular, as follows from Eqs. (60) and (63), the formula for the value ρ^m_2 can be written as $\rho^m_2 = q^*_s/c_0$.

[49] Note that there may be functions $V(\rho)$ and values c_0 that q_{out} in formula (74) exactly equals the flux out from a wide jam. The latter case may be realized for those functions $V(\rho)$ in which a monotonous increase in parameter c_0 brings about a monotonous decrease in the value ρ^m_2 in Eq. (62) in such a way that this value passes through the point of contact of the line $\psi_m(\rho) = V(\rho^m_{\min}) + c_0(1-\rho/\rho^m_{\min})$ and the function $V(\rho)$ at some $c_0 = c^*_0$. At $c_0 = c^*_0$ the line $\psi_m(\rho)$ is obviously tangent to the curve $V(\rho)$, i.e., the value c^*_0 corresponds to a solution of the set of equations $dV/d\rho|_{\rho^m_2} = -c^*_0/\rho^m_{\min}$, $V(\rho^m_2) = V(\rho^m_{\min}) + c^*_0(1-\rho^m_2/\rho^m_{\min})$, $V(\rho^m_2) = V(\rho^m_{\max}) + c^*_0(1-\rho^m_2/\rho^m_{\max})$, and $\rho^m_2 = \sqrt{\rho^m_{\max}\rho^m_{\min}}$. Then, for $c_0 \geqslant c^*_0$, when Eq. (6) is still valid, $\rho_b = \rho^m_{\min}$, i.e., the jam is wide at the boundary point $\rho_h = \rho_b$. In this case, for each density ρ_h in the range $\rho^m_{\min} < \rho_h < \rho_{c1}$, a solution for a narrow unstable jam can be found in addition to a solution for a wide stable jam.

[50] The numerical algorithm of the solution of model Eqs. (1)–(3) was briefly described in Ref. [7].

[51] In the case shown in Fig. 7, the value of flux in the essentially homogeneous traffic flow upstream from a jam is higher than the value of flux in the flow downstream from the jam. For model Eqs. (1)–(3) featuring the cycle boundary conditions (3) to be used in the numerical calculations, the length of the road L was set sufficiently greater ($L = 45$ km) than the length of the section of the road (13 km) where the initial distributions related to the experiment (Fig. 2 in Ref. [7]) were used (Fig. 7). This did not affect the results of numerical calculations, because the jams did not reach the ends of the road ($x = 0$ and $x = L$) during the numerical calculations.

[52] In the examples shown in Figs. 9 and 11, the cyclic boundary condition $\rho(0,t) = \rho(L,t)$ is used, whereas the examples shown in Figs. 10 and 12 correspond to the boundary conditions $\rho(0,t) = \rho_{h1}$ and $\rho(L,t) = \rho_{h2}$, where ρ_{h1}, and ρ_{h2} are constants. A numerical investigation of the LW model showed that the qualitative behavior of jams in the LW model does not depend on the type of boundary conditions.

[53] A. Brenneis, P. Konhäuser, B. S. Kerner, and A. Eberle, *26th AIAA Fluid Dynamics Conference, San Diego, 1995* (American Institute of Aeronautics and Astronautics, Washington, D.C., 1995), Reprint AIAA 99-2230.

[54] S. Godunov, Mat. Sb. **47**, 271 (1959).

[55] J.-P. Lebacque, in *Transportation and Traffic Theory* (Ref. [13]), p. 647; D. D. Bui, P. Nelson, and S. L. Narasimhan, Report No. FHWA/TX-92/1232-7, Texas Transportation Institute, 1992 (unpublished); R. Ansorge, Transp. Res. B **24**, 133 (1990).

[56] A. Brenneis, P. Konhäuser, and B. S. Kerner (unpublished).

[57] Each of these two shock waves corresponds to a tangent to the fundamental diagram $Q(\rho)$: tangent 1 is related to the upstream front, and tangent 2 in Figs. 11(b) and 11(c) is related to the downstream front of the jam. One can see that at some time tangent 2 has a more negative slope in comparison with tangent 1 [Fig. 11(c), $t = 18$ min]. Therefore, the downstream front of the jam overtakes the upstream front, and the jam disappears.